







Olfactory bulb astrocytes link social transmission of stress to cognitive adaptation in male mice

Received: 14 January 2024

Accepted: 6 August 2024

Published online: 18 August 2024

 Check for updates

Paula Gómez-Sotres¹, Urszula Skupio ¹, Tommaso Dalla Tor^{1,2},
Francisca Julio-Kalajzic¹, Astrid Cannich¹, Doriane Gisquet¹,
Itziar Bonilla-Del Rio^{2,3}, Filippo Drago⁴, Nagore Puente^{2,3}, Pedro Grandes^{2,3},
Luigi Bellocchio¹, Arnau Busquets-Garcia ⁵, Jaideep S. Bains ^{6,7,8}  &
Giovanni Marsicano ^{1,8} 

Emotions and behavior can be affected by social chemosignals from conspecifics. For instance, olfactory signals from stressed individuals induce stress-like physiological and synaptic changes in naïve partners. Direct stress also alters cognition, but the impact of socially transmitted stress on memory processes is currently unknown. Here we show that exposure to chemosignals produced by stressed individuals is sufficient to impair memory retrieval in unstressed male mice. This requires astrocyte control of information in the olfactory bulb mediated by mitochondria-associated CB1 receptors (mtCB1). Targeted genetic manipulations, in vivo Ca²⁺ imaging and behavioral analyses reveal that mtCB1-dependent control of mitochondrial Ca²⁺ dynamics is necessary to process olfactory information from stressed partners and to define their cognitive consequences. Thus, olfactory bulb astrocytes provide a link between social odors and their behavioral meaning.

Understanding social signals from conspecifics that portend potential danger can determine the difference between life and death. In humans and nonhuman animals, chemosignals associated with affective states, such as fear^{1,2}, stress^{3,4} or others⁵ can modulate how other individuals perceive and react to the environment. Consistently, alterations of chemosignal processing are present in subjects with social pathologies such as autism spectrum disorders⁶. In rodents, the interaction with an individual previously exposed to threat initiates specific investigative behaviors that enable observers to detect and process stress chemosignals^{7,8}. The processing of this information by an unstressed conspecific results in behavioral and synaptic changes that mirror those observed in the stressed individual. Direct stress also

inhibits certain types of non-stress-related memory, such as delayed alternation memory⁹ and novel object recognition (NOR)^{10,11}. Nevertheless, whether detecting and processing stress chemosignals can also cause cognitive adaptations in unstressed conspecifics has yet to be explored.

The first central processing station of social chemosignals in mammals is the olfactory bulb (OB). Here, odor information is refined before being forwarded to limbic areas, eventually modulating a variety of behaviors. The activity of the olfactory bulb is under the control of many different local cell types, including astrocytes. These cells modulate neuronal transmission^{12–17} affecting the processing of olfactory information, such as odor detection and discrimination^{15–17}.

¹Université de Bordeaux, INSERM, U1215 Neurocentre Magendie, Bordeaux, France. ²Department of Neurosciences, Faculty of Medicine and Nursing, University of the Basque Country UPV/EHU, E-48940 Leioa, Spain. ³Achucarro Basque Center for Neuroscience, Science Park of the UPV/EHU, Leioa, Spain. ⁴Department of Biomedical and Biotechnological Sciences, Section of Pharmacology, University of Catania, Catania 95124, Italy. ⁵IMIM-Hospital del Mar Medical Research Institute, PRBB, Barcelona, Spain. ⁶Krembil Brain Institute, University Health Network, Toronto, ON, Canada. ⁷Hotchkiss Brain Institute and Department of Physiology & Pharmacology, University of Calgary, Calgary, Canada. ⁸These authors jointly supervised this work: Jaideep S. Bains, Giovanni Marsicano. ✉e-mail: Jaideep.Bains@uhn.ca; giovanni.marsicano@inserm.fr

However, little is known about the contribution of these cells in funneling olfactory information into specific behavioral consequences.

Cannabinoid receptors, their endogenous lipid ligands (endocannabinoids) and the machinery for endocannabinoid synthesis and degradation compose the endocannabinoid system, which is involved in many different brain and body functions¹⁸, including olfaction^{19–21}, stress processing^{10,11,22} and cognition^{23,24}. Endocannabinoids regulate olfactory functions in the OB mainly through their action upon type-1 cannabinoid receptors (CB1)^{20,25,26}. CB1 receptors are expressed in several layers of the OB, but their functional characterization has been so far restricted to neurons²⁷. Astrocytes also express low but functionally very important levels of CB1 receptors^{28–31}. The recent discovery of CB1 receptors associated with mitochondria (mtCB1)^{24,32} and their presence in astrocytes^{29,33} has revealed new information linking mitochondria to synaptic and social functions^{33,34}. Moreover, astrocytic mtCB1 receptors control cellular Ca²⁺ dynamics via modulation of the mitochondrial Ca²⁺ uniporter complex (MCU) and its regulatory protein mitochondrial Ca²⁺ uptake 1 subunit (MICU1)³⁴. Thus, CB1 receptors are optimal tools to probe the functions of different cell types and organelles in social investigation, in the detection of affective state-related olfactory signals and eventually in the transmission of stress and its cognitive consequences.

In this study, we investigated the mechanisms and potential cognitive behavioral consequences of chemosignal-dependent social transmission of stress. Using male mice, we found that detection of chemosignals from a stressed demonstrator leads to an impairment of memory retrieval in a naïve observer. Moreover, we show that subpopulations of CB1 receptors present in astrocytes and mitochondria of the observer are specifically required for these effects. Targeted genetic removal of mtCB1 receptors in the astrocytes of the granular cell layer of the OB decreased social investigation of the stressed partner and abolished NOR impairment. Lastly, mtCB1 receptor-dependent control of mitochondrial Ca²⁺ dynamics in OB astrocytes is necessary for social transmission of stress and its cognitive effects. Thus, OB astrocytic mitochondria represent an early and necessary step in the link between social olfaction, emotional contagion and behavioral consequences.

Results

Social olfactory detection of stress impairs object recognition

Pairs of male cage-mates were separated for 5 min, in which one of them (the demonstrator, DEM) was exposed to a foot-shock protocol (stress) or not (neutral). The other (the observer, OBS) was left undisturbed in the home-cage (Fig. 1a,b). After this, the pairs were reunited and allowed to freely interact for 5 min, during which 8 social and non-social behaviors of OBS interacting with stressed (stress OBS) or neutral DEM partners (neutral OBS) were quantified and compared (Supplementary Fig. 1a). As expected⁸, stress OBS mice spent more time engaged in anogenital investigations, body exploration and allogrooming than neutral OBS (Fig. 1c–f and Supplementary Fig. 1c, d). The affective state of the demonstrator (stressed vs neutral) had no effect on several non-social behaviors (Supplementary Fig. 1d) or anxiety-like responses (Supplementary Fig. 1e, f) of OBS mice. These results confirm that the interaction with a previously shocked partner triggers specific patterns of social responses that have been associated to social transmission of stress (STS)⁸. In order to investigate the behavioral relevance of these processes, we next addressed whether this type of social communication exerts a similar impact on cognitive performance as direct stress experience.

Since acute direct stress impairs long-term novel object recognition (NOR) performance in mice^{10,11}, we used this task to test the impact of socially-transmitted stress on cognition. NOR is composed of different phases, such as acquisition, consolidation and retrieval. First, we tested whether STS experience prior (20 min) to NOR acquisition could affect performance in this cognitive test (Fig. 1g). While directly

stressed DEMs were impaired in this test, neither their partners (stress OBS) nor the neutral DEM/OBS couples displayed any deficit in the task (Fig. 1h; Supplementary Fig. 2a). Next, we tested the effect of STS experience prior (20 min) to NOR retrieval (Fig. 1i). As expected, stressed, but not neutral DEM mice, displayed impaired performance in the NOR (Fig. 1j and Supplementary Fig. 2b). Strikingly, impaired NOR retrieval was also evident in stress OBS, but not in neutral ones (Fig. 1j and Supplementary Fig. 2b), demonstrating that the cognitive impact of socially-transmitted stress is similar to that of direct stress experience itself. These data indicate that STS during acquisition does not alter NOR performance, but the same experience before retrieval induces the same cognitive impairment as direct stress.

These results suggest that a temporal effect might exist in the STS impact on NOR performance. Therefore, we tested if the effect of STS on memory retrieval was still present if STS occurred 6 h before the retrieval phase of the task. Interestingly, neither neutral nor stressed OBS mice showed alterations in NOR performance (Supplementary Fig. 2c). Next, we asked whether this cognitive effect of STS extended to other forms of cognition, such as social memory (Supplementary Fig. 2f). Similarly to NOR, an STS experience prior to retrieval fully abolished social preference for an unfamiliar individual (Supplementary Fig. 2d–f). Thus, the cognitive effects of STS are time-dependent over the course of the memory processing, and they apply to different forms of recognition memory.

Non-volatile chemosignals released from the anogenital region are necessary and sufficient for the synaptic changes triggered by socially-transmitted stress⁸. To start addressing whether similar olfactory cues were involved in the STS-induced NOR impairment, we separated DEM/OBS couples during the STS protocol preceding NOR retrieval with a plexiglass transparent barrier with holes (Fig. 1k). Stress OBS were not impaired in NOR performance (Fig. 1l; Supplementary Fig. 2g), indicating that this separation impeded the specific transmission of information required for the cognitive impairment induced by STS. Considering that the barrier allowed all sensory cues except for direct physical contact, these results suggest that a non-visual, non-auditory and non-volatile cue is required for the STS cognitive effects. As anogenital olfactory cues are sufficient for synaptic effects of STS⁸, we asked whether these chemosignals were also able to elicit the NOR impairment observed in mice after social interaction with stressed partners (Fig. 1m). Direct contact with a cotton swab that was saturated with anogenital secretions of a stressed mouse was sufficient to impair NOR performance (Fig. 1n; Supplementary Fig. 2h). In contrast, exposure to a cotton swab impregnated with the anogenital secretions of a naïve mouse did not alter NOR retrieval as compared to a cotton swab infused with saline (Fig. 1n; Supplementary Fig. 2h). Importantly, the differential effects of the odorants were not linked to the time of exposure (Supplementary Fig. 2i–j). Indeed, a short experience (2–3 s) of stress chemosignals was sufficient to impair NOR performance in mice. Together, these results show that anogenital investigation of stressed mice results in the detection of specific chemosignals that alter memory retrieval, indicating that olfactory processes can link social emotional information to cognitive functions.

Astrocytic and mitochondrial CB1 receptors are required for social anogenital investigation of a stressed partner

CB1 receptors are involved in memory processes, olfaction, stress-induced amnesia and social interactions^{10,20,33}, suggesting the potential involvement of the endocannabinoid system in social olfaction resulting in the transmission of stress and its cognitive effects. To start addressing this hypothesis, we first used a battery of mutant mouse lines lacking CB1 receptors in different cellular and subcellular populations. Observer CB1 mutant male mice were housed immediately after weaning with sex and age-matched demonstrators (see Methods for more details). In comparison to wild-type littermates, OBS mice with a global deletion of CB1 receptors (CB1-KO mice)³⁵ spent less time

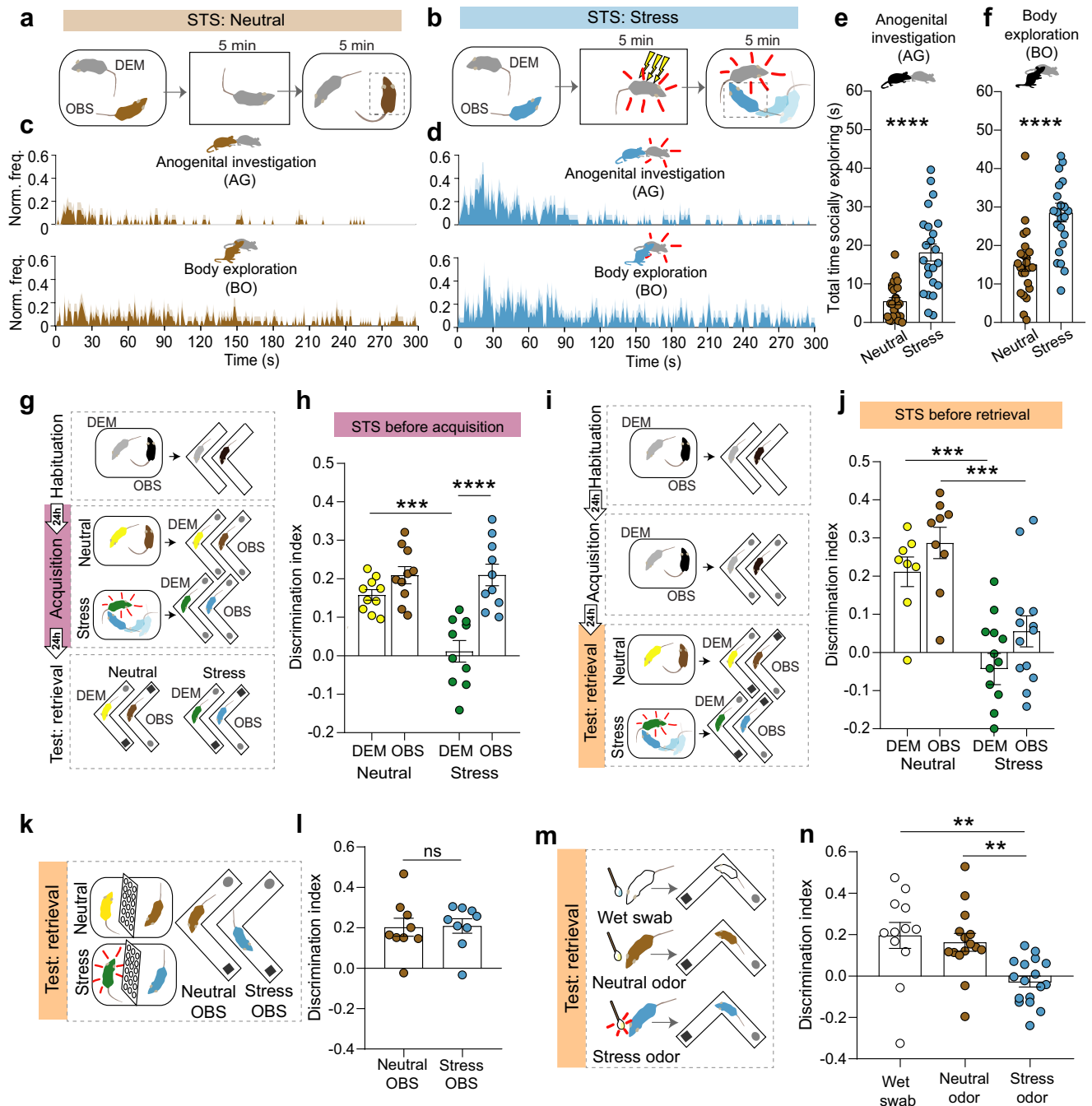


Fig. 1 | Social olfactory detection of stress impairs object recognition performance. **a** Neutral condition of the social transmission of stress (STS) protocol. OBS observer. DEM, demonstrator. **b** Stress condition of the STS protocol. **c** Normalized frequency of anogenital investigation (AG) and body exploration (BO) of OBS mice towards neutral DEM. **d** Normalized frequency AG and BO of OBS mice towards stress DEM. **e** Total time of AG of neutral or stress OBS mice. Two-tailed unpaired Student's *t* test, $p < 0.0001$. **f** Total time of BO of neutral or stress OBS mice. Two-tailed unpaired Student's *t* test, $p < 0.0001$ for both. For (**c–f**), $n_{(\text{neutral})} = 24$, $n_{(\text{stress})} = 23$. **g** Behavioral protocol to assess STS effects in novel object recognition (NOR) acquisition. **h** Discrimination index in the NOR of mice that underwent STS before acquisition. Two-way ANOVA, interaction, $p = 0.0038$, Bonferroni post hoc, $p(\text{neutral DEM vs stress DEM}) = 0.0006$, $p(\text{neutral OBS vs stress DEM}) < 0.0001$, $n = 10$. **i** Behavioral protocol to assess STS effects in NOR retrieval. **j** Discrimination index in the NOR of mice that underwent STS before retrieval. Two-way ANOVA,

effect of STS condition, $p < 0.0001$, Bonferroni post hoc, $p(\text{DEM neutral vs DEM stress}) = 0.0003$, $p(\text{OBS neutral vs OBS stress}) = 0.0007$, $n_{(\text{neutral DEM})} = 13$, $n_{(\text{neutral OBS})} = 8$, $n_{(\text{stress DEM})} = 9$, $n_{(\text{stress OBS})} = 13$. **k** Behavioral protocol to assess sensory cue specificity in STS-induced NOR changes. **l** Discrimination index in the NOR test of barrier-separated OBS mice. $n = 9$. **m** Behavioral protocol to assess odor transmission of stress and subsequent NOR effects. **n** Discrimination index in the NOR test of naive mice after being exposed to a saline wet swab, an odor of a neutral DEM (neutral odor) or from a stressed DEM (stress odor). Ordinary one-way ANOVA, $p = 0.0002$. Bonferroni post hoc, $p(\text{wet swab vs stress odor}) = 0.0025$, $p(\text{neutral odor vs stress odor}) = 0.0066$, $n_{(\text{wet swab})} = 12$, $n_{(\text{neutral odor})} = 15$, $n_{(\text{stress odor})} = 17$. Data are expressed in mean \pm SEM. * $p < 0.05$, ** $p < 0.01$, *** $p < 0.001$, **** $p < 0.0001$. For detailed statistical information, see Supplementary Table 1. Source data are provided as a Source Data file.

engaged in anogenital investigations of a stressed partner (Fig. 2a, c, d). A similar phenotype was observed in OBS mice lacking CB1 from cortical glutamatergic neurons (Glu-CB1-KO)³⁶, astrocytes (GFAP-CB1-KO)³⁷ and mitochondria (DN22-CB1-KI)³⁸ but not from forebrain GABAergic neurons (GABA-CB1-KO)³⁶ (Fig. 2a, c, d). Some of these alterations did not appear to be specific for anogenital investigations. Global CB1-KO and Glu-CB1-KO displayed other changes in social behavior, such as a decrease in body exploration (Fig. 2b, e, f) and/or allogrooming (Supplementary Fig. 3a). Conversely, the GFAP-CB1-KO and DN22-CB1-KI lines displayed a specific decrease of anogenital interactions with no other changes in social or other recorded behaviors (Fig. 2b, e, f and Supplementary Fig. 3a). Importantly, no genotype effect was detected in the social behaviors during interactions with neutral DEM mice (Supplementary Fig. 3b–f), indicating that the mutations did not alter the basal ability of the mice to express these innate behaviors. Altogether, these data show that anogenital investigations specifically linked to the presence of a stressed partner are controlled by CB1 receptors located in astrocytes and mitochondria, suggesting that these cells and these organelles might be the sites where the endocannabinoid system controls social transmission of stress.

Mitochondrial CB1 receptors in astrocytes of the olfactory bulb are required for anogenital investigation and subsequent cognitive impairment

Social transmission of stress depends on olfactory cues⁸ and the data collected so far show that exposure to odors from the anogenital region of stressed mice is sufficient to impair NOR retrieval.

As astrocytic and mitochondrial CB1 receptors appear to be necessary specifically for anogenital investigation, and considering that the first brain region devoted to the processing of chemosignals is the olfactory bulb (OB), we asked whether mitochondrial CB1 (mtCB1) receptors in astrocytes of this brain region might be responsible for STS and its cognitive consequences. As the anatomical presence of mtCB1 receptors in OB astrocytes has not been demonstrated, we performed immunoelectron microscopy to detect CB1 receptors in immunoperoxidase-stained astrocytes in the mouse OB granular cell layer (GCL) (Fig. 3a). In addition to excitatory and inhibitory synaptic terminals²⁶, CB1 immunoparticles were localized to astrocytic plasma membranes and mitochondria (mtCB1) of wildtype mice (Fig. 3b, c). This labeling was not observed in CB1-KO mice (Fig. 3e).

To address the functional role of mtCB1 receptors in STS and its cognitive consequences, we adopted a double viral approach in CB1-flox mice³⁹ (Fig. 3f), using Cre expression both to delete and to re-express wild-type or mutant CB1 receptors^{11,24,38}. Thus, we generated four groups of OB-CB1 mutant mice (see Methods for details; Fig. 3f): (i) control mice (Ctrl), expressing the CB1 receptor in a wild-type fashion, (ii) OB-GFAP-CB1-KO mice, lacking the receptor in OB astrocytes, (iii) OB-GFAP-CB1-RS (rescue) mice, carrying deletion of endogenous CB1 in OB astrocytes and re-expression of a wild-type form of the CB1 protein in the same cells, and (iv) OB-GFAP-DN22-RS mice carrying deletion of endogenous CB1 in OB astrocytes and re-expression of the mutant DN22-CB1, lacking 22 aminoacids of the original CB1 gene in the same cells, thereby excluding mitochondrial association^{24,38} (Fig. 3g). In OB-GFAP-CB1-RS and OB-GFAP-DN22-RS, CB1 and DN22-CB1 constructs were respectively expressed to similar levels, mostly in the granular cell layer of the olfactory bulb (Fig. 3h) and with astrocytic specificity of expression of around 82% for both constructs (calculated as the percentage of infected cells co-localizing with the astrocytic marker GFAP; Fig. 3h, i).

First, we tested the behavior of these mutants in the NOR task under naïve or acute stress conditions (Supplementary Fig. 4a, b). OB-GFAP-CB1-KO, OB-GFAP-CB1-RS and OB-GFAP-DN22-RS mice displayed similar NOR performance as Ctrl animals (Supplementary Fig. 4a, b). They also showed the expected impairment in NOR following direct

foot-shock (Supplementary Fig. 4a, b). To assess whether these genetic manipulations in the OB could alter general olfaction, we tested the mutant mice in different olfactory tests. First, we observed no differences between controls and OB-GFAP-CB1-KO mutant mice in the buried food test⁴⁰ (Supplementary Fig. 4c). Moreover, the deletion of CB1 receptors in OB astrocytes did not alter social interactions with an unfamiliar naïve mouse (Supplementary Fig. 4d) or with a neutral DEM (Supplementary Fig. 4e, f). Finally, OB-GFAP-CB1-KO were able to discriminate between different neutral odors (Supplementary Fig. 4g) and displayed no deficits in odor detection (Supplementary Fig. 4h). Thus, these genetic manipulations did not alter NOR performance, its impairment by direct stress, social interactions or general olfactory functions. This indicates that the approach is suitable to study the specific functions of astrocytic mtCB1 receptors in the OB in STS and its cognitive consequences.

The deletion of CB1 receptors in OB astrocytes (OB-GFAP-CB1-KO) in stress OBS mice led to a decrease of anogenital investigation (Fig. 3j–l), which was fully restored by the re-expression of wild-type CB1 in OB astrocytes (OB-GFAP-CB1-RS; Fig. 3j–l). Notably, however, the re-expression of the mutant protein DN22-CB1 (OB-GFAP-DN22-RS) was not sufficient to rescue this phenotype (Fig. 3j–l). During social transmission of stress, no OB-GFAP-CB1 mutant group displayed any other alteration in social (body exploration or allogrooming, Supplementary Fig. 4i, j) or non-social behaviors (Supplementary Fig. 4i). Altogether, these data indicate that the anogenital exploration of a stressed partner, which is crucial for social transmission of stress, requires the presence of CB1 receptors associated with mitochondrial membranes in OB astrocytes.

Next, we asked whether this specific subpopulation of CB1 receptors also participates in the impairment of NOR retrieval following STS. OB-GFAP-CB1-KO mice were immune to the NOR-impairing effect of STS (Fig. 3m, Supplementary Fig. 4k) or of a short or long exposure to a swab impregnated with anogenital secretions from a stressed partner (Supplementary Fig. 4l, m). This effect of STS was fully restored in OB-GFAP-CB1-RS (Fig. 3m, Supplementary Fig. 4k). However, exclusion of CB1 receptors from astrocytic mitochondria in OB-GFAP-DN22-RS mice protected from the consequences of transmitted stress to a similar extent as the complete deletion of astrocytic CB1 in OB-GFAP-CB1-KO mice (Fig. 3m, Supplementary Fig. 4k). The anatomical data shown in Fig. 3h indicate that Cre-dependent recombination using *AAV-GFAP-Cre* mice in the OB involves about 20% of non-GFAP-positive cells, which are presumably neurons. Therefore, it is possible that the phenotypes of the mutant mice are linked to genetic alterations in these cells. To test this possibility, we injected a neuronal specific AAV (*AAV-Syn-Cre*) into the OB of CB1-flox mice (Supplementary Fig. 5a) and evaluated their social behavior and subsequent NOR performance. This manipulation did not alter anogenital investigation or body exploration (Supplementary Fig. 5b, c), nor did it affect the impairment of NOR retrieval following stress transmission (Supplementary Fig. 5d, e). Collectively, these results indicate that mtCB1 receptors in OB astrocytes are necessary for specific social olfactory behaviors required for STS and its impact on NOR.

Mitochondrial Ca²⁺ dynamics in olfactory bulb astrocytes is required for social processing of stress chemosignals

Astrocytic mtCB1 receptors modulate the entry of Ca²⁺ into mitochondria via regulation of ER-mitochondrial Ca²⁺ transfer³⁴. Our data suggests that processing of stress social chemosignal in the OB by astrocytic mtCB1 receptors is required for appropriate behavioral consequences. Thus, we hypothesized that mitochondrial Ca²⁺ increase in OB astrocytes might be triggered by social transmission of stress and mediate its impact on NOR performance. We tested whether the detection of a stress chemosignal was associated with dynamic changes in mitochondrial Ca²⁺ levels of OB astrocytes of behaving animals. We expressed a mitochondrial-targeted genetic Ca²⁺ indicator

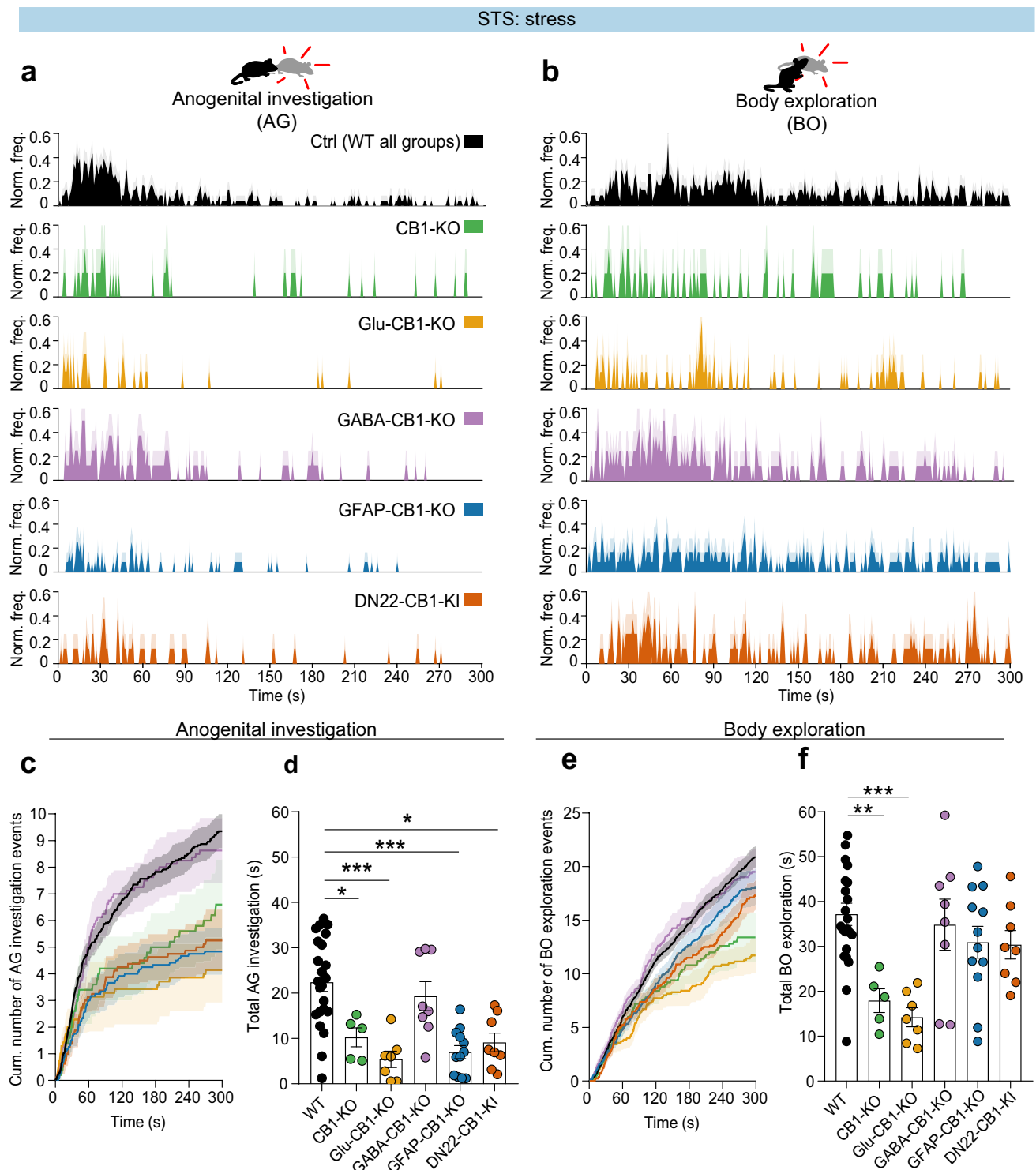
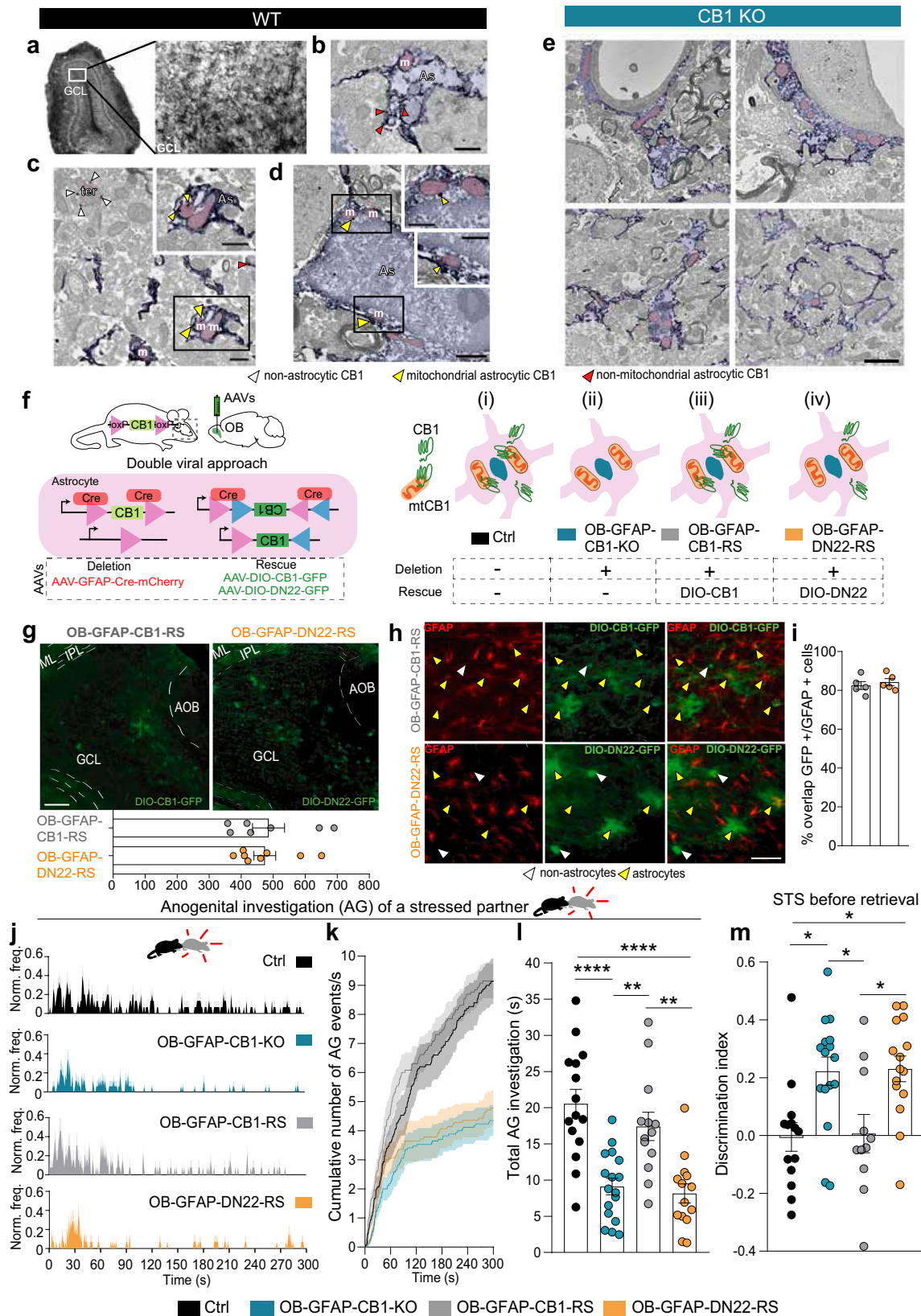


Fig. 2 | Astrocytic and mitochondrial CB1 receptors are specifically required for anogenital investigation of a stressed partner. **a** Normalized frequency of anogenital investigation (AG) of global or conditional CB1 mutant OBS over 5 min social interaction with a WT familiar stress DEM. Ctrl mice include WT of all groups (not significantly different). Mutant mice are CB1-KO, Glu-CB1-KO, GABA-CB1-KO, GFAP-CB1- and DN22-CB1-KI. **b** Normalized frequency of body exploration (BO) of global or conditional CB1 mutant OBS over 5 min social interaction with a WT familiar stress DEM. **c** Cumulative number of AG events of global or conditional CB1 mutant OBS during 5 min social interaction with a stress DEM. **d** Total time of AG of a stress DEM by global or conditional CB1 mutant OBS during 5 min social interaction. Ordinary one-way ANOVA, $p < 0.0001$. Bonferroni post hoc, p (WT vs CB1-KO) =

0.0111, p (WT vs Glu-CB1-KO) < 0.0001 , p (WT vs GFAP-CB1-KO) < 0.0001 , p (WT vs DN22-CB1-KI) = 0.0005. **e** Cumulative number of BO events of global or conditional CB1 mutant observer mice during 5 min social interaction with a stress DEM. **f** Total time of BO of a stress DEM by global or conditional CB1 mutant observer mice during 5 min social interaction. Ordinary one-way ANOVA, $p = 0.0002$. Bonferroni multiple comparisons, p (WT vs CB1-KO) = 0.005, p (WT vs Glu-CB1-KO) < 0.0001 . $n_{(WT)} = 23$, $n_{(CB1-KO)} = 5$, $n_{(Glu-CB1-KO)} = 7$, $n_{(GABA-CB1-KO)} = 8$, $n_{(GFAP-CB1-KO)} = 12$, $n_{(DN22-CB1-KI)} = 8$. Data are expressed in mean \pm SEM. * $p < 0.05$, ** $p < 0.01$, *** $p < 0.001$. For detailed statistical information, see Supplementary Table 1. Source data are provided as a Source Data file.



(mitoGcAMP6s³⁴) in the astrocytes of the OB of naïve mice (Fig. 4a–d). Using fiber photometry, we then recorded mitochondrial Ca²⁺ signals of mice responding to successive and counterbalanced exposures to a cotton swab impregnated either with saline (hereafter called “wet swab”), or with anogenital secretions of a stressed familiar individual (hereafter called “stress odor”), or with the anogenital secretions of a

neutral familiar individual (hereafter “neutral odor”). All olfactory exposures induced an increase in the levels of mitoGcAMP6s fluorescence. However, olfactory bulb astrocytic mitochondria were more responsive to stress odor than to a wet swab or a neutral odor (Fig. 4e–h), suggesting that mitochondrial Ca²⁺ transients are specifically involved in the processing of stress chemosignals, but not other

Fig. 3 | Mitochondrial CB1 receptors in astrocytes of the olfactory bulb are required for social processing of stress chemosignals. **a** Localization of CB1 and GLAST in granular cell layer (GCL) of WT mice by electron microscopy. **b** CB1 labeling in an astrocyte membrane (As, purple). Scale bar, 0.5 μm . **c** CB1 particles in synaptic terminals (ter), astrocytes (As) and mitochondria (m). Low magnification scale bar, 1 μm ; high magnification bar, 0.5 μm . **d** CB1 particles in astrocytic mitochondria. Low magnification scale bar, 1 μm ; high magnification bar, 0.5 μm . **e** Lack of CB1 receptor signal in astrocytes and mitochondria in GCL of CB1-KO. Scale bar, 1 μm . **f** Viral strategy to genetically manipulate specific subcellular CB1 receptor populations in astrocytes of the olfactory bulb (OB). **g** Above, viral expression of endogenous fluorescence of the AAV-DIO-CB1-GFP and AAV-DIO-DN22-GFP in the granular cell layer, GCL, of the OB. Scale bar, 250 μm . Below, relative fluorescence of both viruses. **h** Immunostaining against GFAP, endogenous fluorescence (green) of the AAV-DIO-CB1-GFP (top) and AAV-DIO-DN22-GFP (bottom) and merge in the GCL of the OB. Scale bar, 50 μm . **i** Percentage of overlap between GFAP-positive cells and AAV-driven GFP expressing cells. **j** Normalized frequency of anogenital

investigation (AG) events of stress OB-GFAP-CB1 mutant OBS. **k** Cumulative number of AG events of stress OB-GFAP-CB1 mutant OBS. **l** Total AG of a stress OB-GFAP-CB1 mutant OBS. Ordinary one-way ANOVA, $p < 0.0001$. Bonferroni post hoc, $p(\text{Ctrl vs OB-GFAP-CB1-KO}) < 0.0001$, $p(\text{Ctrl vs OB-GFAP-DN22-RS}) < 0.0001$, $p(\text{OB-GFAP-CB1-RS vs OB-GFAP-CB1-KO}) = 0.0032$, $p(\text{OB-GFAP-CB1-RS vs OB-GFAP-DN22-RS}) = 0.0015$. **m** Discrimination index in the NOR of stress OB-GFAP-CB1 mutant OBS. Ordinary one-way ANOVA, $p = 0.0009$. Bonferroni post hoc, $p(\text{Ctrl vs OB-GFAP-CB1-KO}) = 0.0129$, $p(\text{Ctrl vs OB-GFAP-DN22-RS}) = 0.0109$, $p(\text{OB-GFAP-CB1-RS vs OB-GFAP-CB1-KO}) = 0.361$, $p(\text{OB-GFAP-CB1-RS vs OB-GFAP-DN22-RS}) = 0.0303$. For (a–e), $n = 3$ individual mice for each WT and KO. For (g), $n_{(\text{OB-GFAP-CB1-RS})} = 7$, $n_{(\text{OB-GFAP-DN22-RS})} = 8$ mice for each AAV. For (h, i), $n = 5$ individual mice. For (j, k, l) $n(\text{Ctrl}) = 15$, $n(\text{OB-GFAP-CB1-KO}) = 17$, $n(\text{OB-GFAP-CB1-RS}) = 13$, $n(\text{OB-GFAP-DN22-RS}) = 14$. For m, $n(\text{Ctrl}) = 14$, $n(\text{OB-GFAP-CB1-KO}) = 16$, $n(\text{OB-GFAP-CB1-RS}) = 11$, $n(\text{OB-GFAP-DN22-RS}) = 15$. Data are expressed in mean \pm SEM. * $p < 0.05$, ** $p < 0.01$, *** $p < 0.001$, **** $p < 0.0001$. For detailed statistical information, see Supplementary Table 1. Source data are provided as a Source Data file.

anogenital odorants. Moreover, other non-social neutral odors like banana and almond (isoamyl acetate and benzaldehyde, respectively) did not elicit mitochondrial responses significantly different from wet swab exposure (Supplementary Fig. 6a–c), further supporting the specific involvement of mitochondrial Ca^{2+} dynamics in the processing of social stress odors. As differences in mitochondrial Ca^{2+} can reflect changes in cytosolic Ca^{2+} levels⁴¹, we measured cytosolic Ca^{2+} responses to different odors in mice expressing GcAMP6f in the astrocytes of the granular cell layer of the OB (Supplementary Fig. 6d–g). Surprisingly, no differences were observed in the cytosolic responses to wet swab or stress odor (Supplementary Fig. 6h, i), suggesting that mitochondrial Ca^{2+} uptake plays a specific and active role in the processing of stress social odors.

Altogether, these data suggest that changes in mitochondrial Ca^{2+} levels are dynamically involved in the processing of STS information needed for its cognitive consequences. Astrocytic mtCB1 receptors are involved in the activation of the mitochondrial Ca^{2+} uniporter (MCU) channel through the phosphorylation of the regulatory protein MICU1 (ref. 42.), eventually determining the impact of astrocytes on synaptic functions³⁴. Mitochondrial CB1 activation is known to regulate Akt-mediated phosphorylation of MICU1 at the serine 124, allowing the opening of the MCU and thereby favoring mitochondrial Ca^{2+} entry^{34,43}. To determine whether mitochondrial Ca^{2+} entrance is necessary for STS and its cognitive consequences, we manipulated these processes by expressing a non-phosphorylatable dominant negative form of MICU1 (MICU^{S124A}; ref. 34, Fig. 4i–k) in the astrocytes of the OB of wild-type mice. Mice over-expressing MICU^{S124A} in OB astrocytes (AAV-GFAP-MICU^{S124A}) and their corresponding controls over-expressing MICU^{WT} (AAV-GFAP-MICU^{WT}) were tested in the stress transmission-NOR protocol (Fig. 4i–k). As compared to control littermates, mice injected with AAV-GFAP-MICU^{S124A} engaged in less anogenital contact with their stressed partners (AAV-GFAP-MICU^{WT}) (Fig. 4l–n), without any changes in body exploration (Supplementary Fig. 7a), allogrooming or other nonsocial behaviors (Supplementary Fig. 7b). Notably, mice carrying the dominant negative form of MICU1 in OB astrocytes lacked the STS-induced impairment of NOR retrieval (Fig. 4o and Supplementary Fig. 7c, d). These mutant mice (i) displayed normal social behaviors during interactions with neutral DEM partners (Supplementary Fig. 7e, f); (ii) were not impaired in NOR performance after interaction with a neutral DEM mouse (Supplementary Fig. 7g–i); and (iii) were able to normally retrieve buried food pellets (Supplementary Fig. 7j). Thus, mitochondrial Ca^{2+} transients in OB astrocytes are not involved in basal social interactions, cognitive performance and olfactory abilities, but they play a specific causal role in STS and its cognitive consequences.

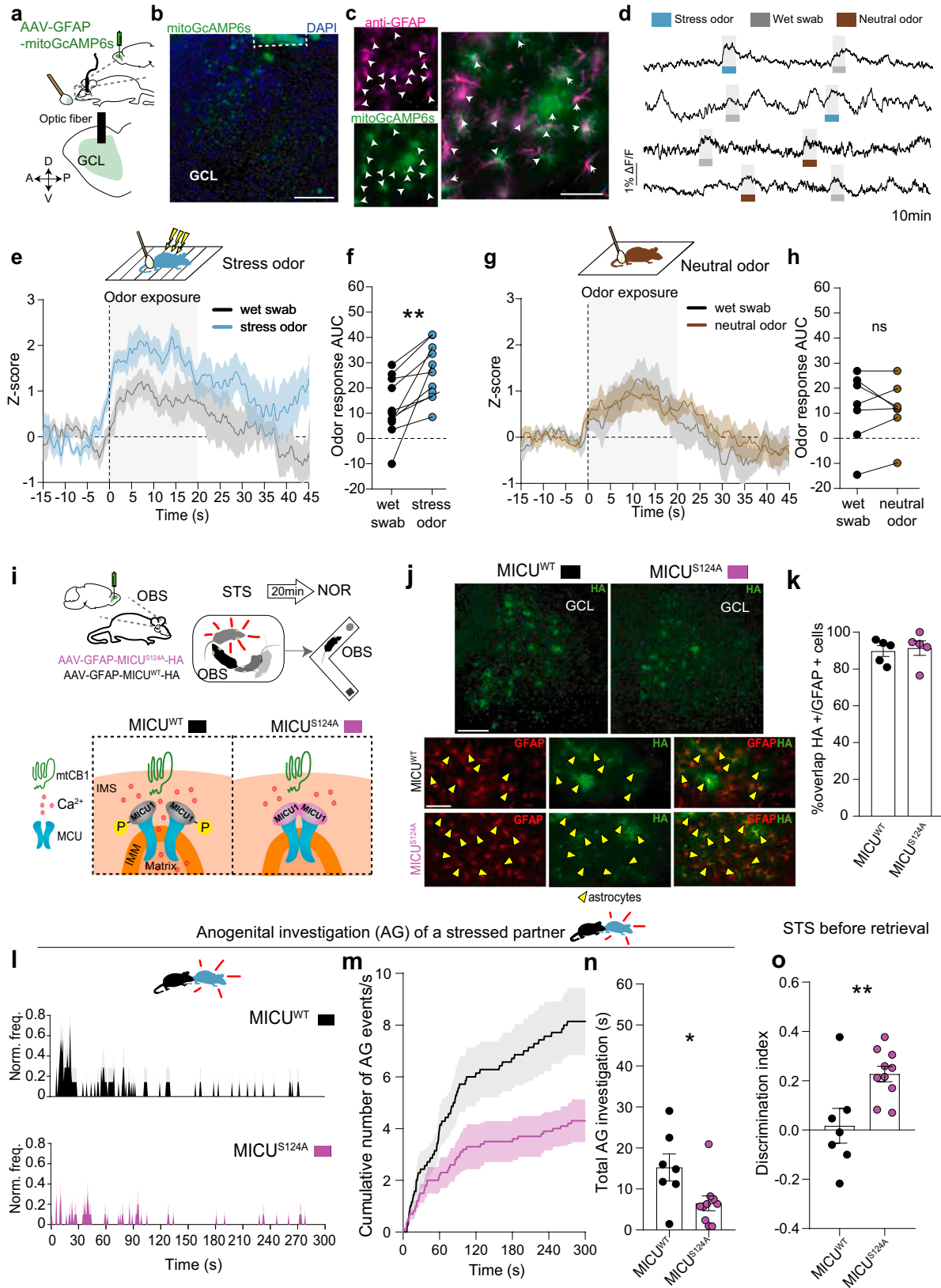
The data obtained so far indicate that mtCB1 in OB astrocytes and the control of mitochondrial Ca^{2+} dynamics are causally involved

in the processes mediating STS and its cognitive consequences. However, these data do not exclude the possibility that these two phenomena might act independently. Therefore, we next investigated the causal relationship between OB astrocyte mtCB1 receptors and stress-social odor-induced mitochondrial Ca^{2+} dynamics. We expressed mitoGcAM6s in Ctrl, OB-GFAP-CB1-KO, OB-GFAP-CB1-RS and OB-GFAP-DN22-RS mice (Fig. 5a, b). None of these mice displayed differential responses to neutral odors as compared to wet swabs (Fig. 5c, e). As expected, however, Ctrl mice responded to the stress odor with higher dynamic increase of Ca^{2+} levels as compared to the wet swab (Fig. 5d, f). This effect was fully abolished in OB-GFAP-CB1-KO (Fig. 5d, f), indicating that activation of CB1 receptors in OB astrocytes is causally linked to mitochondrial Ca^{2+} responses induced by stress social odors. This phenotype was fully rescued in OB-GFAP-CB1-RS mice re-expressing wild-type CB1 receptors (Fig. 5d, f), but not in OB-GFAP-DN22-RS mice lacking mitochondrial localization of the CB1 receptor (Fig. 5d, f). These results show that astrocytic mtCB1 receptors are required for mitochondrial Ca^{2+} responses determining the specific processing of social stress chemosignals. Thus, a direct causal chain of events likely links exposure to stress social odors, activation of mtCB1 receptors in OB astrocytes, mitochondrial Ca^{2+} uptake and social transmission of stress and its cognitive consequences.

Discussion

This study demonstrates functional links between social transmission of stress, olfactory processing and cognitive alterations in male mice. These links depend on the endogenous activation of CB1 receptors located in astrocytic mitochondria of the olfactory bulb and on the consequent control of Ca^{2+} signaling by these organelles. We found that detection of stress-induced chemosignals by naïve observers impairs object and social recognition memory retrieval to a similar extent as direct stress experience. Mitochondrial CB1 receptors in OB astrocytes are required for changes in mitochondrial Ca^{2+} uptake leading to the impairment of cognitive performance induced by social transmission of stress. Thus, smelling certain odors has the ability to override unrelated cognitive processes.

Our data indicate that strong similarities exist between the cognitive effects of direct foot-shock stress and STS. Indeed, the effects of direct or socially-transmitted stress during retrieval of NOR memory are virtually undistinguishable. However, important differences exist. Obviously, as discussed below, the sensory perception processes involved are fully different (somatosensory for direct stress and olfactory for STS). Another less expected difference is that, whereas direct stress equally worsens different phases of NOR memory^{10,11}, STS impairs this cognitive task only when experienced right before retrieval, but not when the delay is longer or prior to acquisition. There is no



current explanation for this apparent discrepancy and future studies will address this interesting point. However, recent data from our laboratory showed that, although stress and corticosteroid treatments affect different phases of NOR memory equally, the neurocircuitry mechanisms involved are different¹¹. This suggests that distinct stress-like experiences (direct, STS or others) differentially impact selective

neurocircuitries, resulting in specific modulation of cognitive processes.

By showing that mtCB1 receptors in astrocytes of the OB are necessary for anogenital investigation of a shocked DEM and the subsequent NOR deficit, our data indicate that refined control of olfactory processes underlie the effects of STS. However, how can OB

Fig. 4 | Mitochondrial Ca²⁺ dynamics in OB astrocytes are required for stress chemosignal processing and subsequent behavioral adaptations. **a** Experimental approach to record mitoCa²⁺ in astrocytes of the olfactory bulb (GCL, granular cell layer). **b** Representative images showing fiber placement, mitoGcAMP6s endogenous fluorescence and DAPI. Scale bar, 250 μm. *n* = 7 individual mice. **c** MitoGcAMP6s endogenous fluorescence and immunostaining for GFAP and endogenous fluorescence. 98.65% of mitoGcAMP6s-positive cells do contain GFAP, *n* = 7. Scale bar, 50 μm. **d** Representative mitoCa²⁺ signal traces of animals expressing mitoGcAMP6s in the astrocytes of the olfactory bulb. **e** Z-scored ΔF/F mitoCa²⁺ responses in OB astrocytes aligned to the onset of the first contact with the odorant stimulus (wet swab and stress odor). *n* = 10 individual mice. **f** Z-scored AUC of mitoCa²⁺ signals during wet swab and stress odor exposure. Two tailed paired Student's *t* test, *p* = 0.0034. *n* = 10. **g** Z-scored ΔF/F mitoCa²⁺ responses in OB astrocytes to wet swab and neutral odor. *n* = 7 individual mice. **h** Z-scored AUC of mitoCa²⁺ signals during wet swab and neutral odor exposure. *n* = 7. **i** Viral

strategy to manipulate mitoCa²⁺ uptake in astrocytes of the olfactory bulb of wild-type C57BL/6-N mice that were then used as OBS during STS and NOR. **j** Top, virally-induced HA expression in the GCL of the OB. Bottom, immunostaining against HA and GFAP. Scale bars are 150 μm (top) and 50 μm (bottom). *n* = 7 individual mice. **k** Percentage of overlap between GFAP-positive cells and AAV-driven HA expressing cells. *n* = 5 mice for each virus. **l** Normalized frequency of AG events of MICU1 stress OBS mice. **m** Cumulative number of AG events of MICU1 stress OBS mice. Two-tailed unpaired Mann-Whitney test, *p* = 0.025. **n** Discrimination index in the NOR test of MICU1 OBS mice after socializing with a stress DEM. Two-tailed unpaired Student's *t* test, *p* = 0.0086. For (l-o), *n* (MICU1^{WT}) = 7, *n* (MICU1^{S124A}) = 10. Data are expressed in mean ± SEM. **p* < 0.05, ***p* < 0.01. For detailed statistical information, see Supplementary Table 1. Source data are provided as a Source Data file. MCU mitochondrial Ca²⁺ uniporter, IMS intermembrane mitochondrial space, IMM intramembrane mitochondrial space.

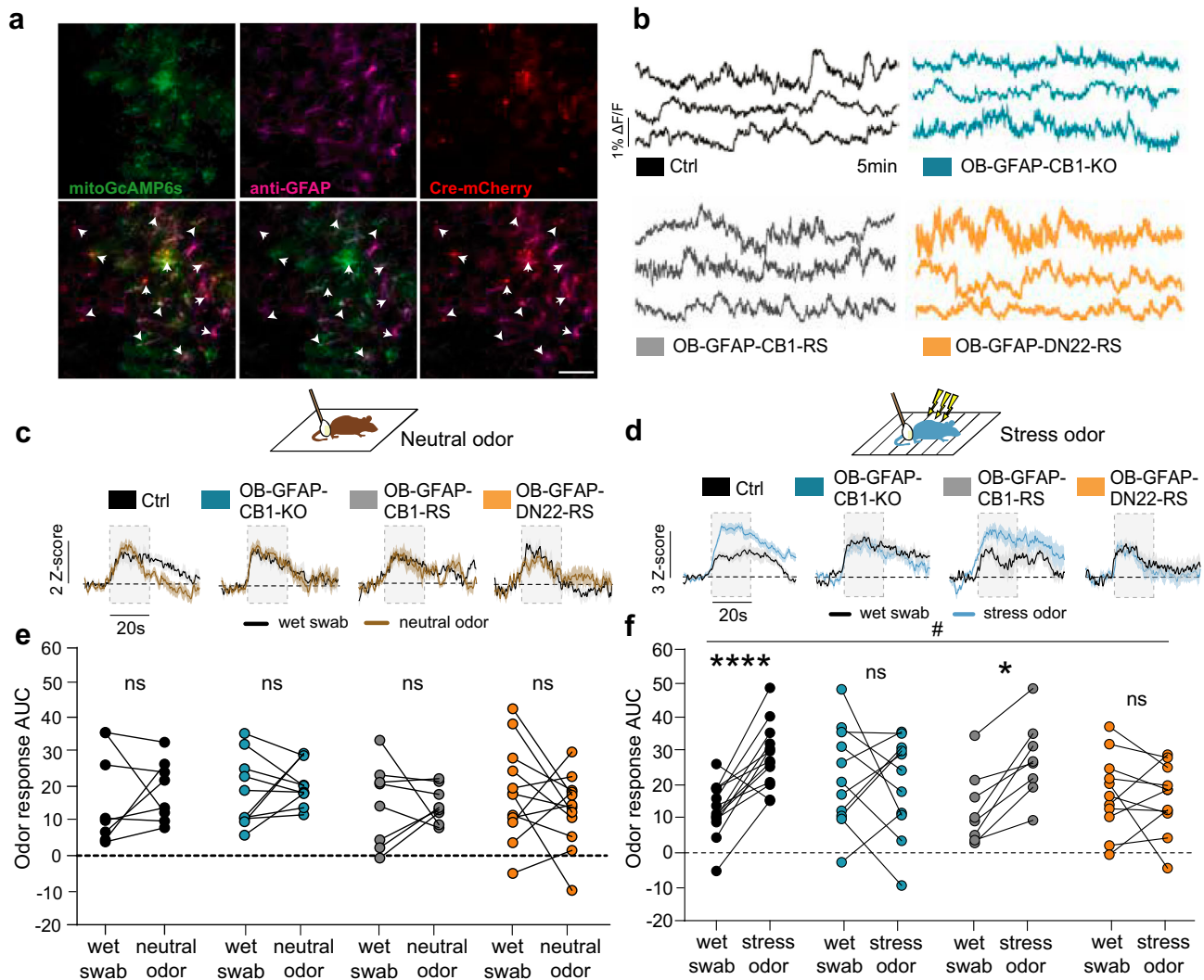


Fig. 5 | Mitochondrial Ca²⁺ responses in OB astrocytes to stress chemosignals require astrocytic mtCB1 receptors. **a** Representative images showing mitoGcAMP6s endogenous fluorescence (green), Cre endogenous fluorescence resulting from the AAV-GFAP-Cre-mCherry injection (red) and immunostaining for GFAP (purple). Scale bar, 50 μm, *n*_(OB-GFAP-CB1-KO) = 7. **b** Representative mitoCa²⁺ signal traces of OB-GFAP-CB1 mutant mice expressing mitoGcAMP6s in OB astrocytes. **c** Z-scored ΔF/F mitoCa²⁺ responses in astrocytes of the olfactory bulb of OB-GFAP-CB1 mutant mice aligned to the onset of the odor exposure to a wet swab or a swab impregnated with odor of a neutral partner. Rectangle represents the time of odor exposure used to calculate AUC. *n* (Ctrl) = 8, *n* (OB-GFAP-CB1-KO) = 10, *n* (OB-GFAP-CB1-RS) = 8, *n* (OB-GFAP-DN22-RS) = 12. **d** Z-scored ΔF/F mitoCa²⁺ responses in astrocytes of the

olfactory bulb of OB-GFAP-CB1 mutant mice aligned to the onset of the odor exposure to a wet swab or a stress odor. *n* (Ctrl) = 13, *n* (OB-GFAP-CB1-KO) = 11, *n* (OB-GFAP-CB1-RS) = 8, *n* (OB-GFAP-DN22-RS) = 11. **e** Z-scored mitoCa²⁺ signal AUC from wet swab and neutral odor exposures from OB-GFAP-CB1 mutant mice. *n* (Ctrl) = 8, *n* (OB-GFAP-CB1-KO) = 10, *n* (OB-GFAP-CB1-RS) = 8, *n* (OB-GFAP-DN22-RS) = 12. **f** Z-scored mitoCa²⁺ signal AUC from wet swab and stress odor exposures from OB-GFAP-CB1 mutant mice. Two tailed paired Student's *t* test, *p* (Ctrl) = 0.0002, *p* (OB-GFAP-CB1-RS) = 0.0013, *n* (Ctrl) = 13, *n* (OB-GFAP-CB1-KO) = 11, *n* (OB-GFAP-CB1-RS) = 8, *n* (OB-GFAP-DN22-RS) = 11. Data are expressed in mean ± SEM. **p* < 0.05, *****p* < 0.0001. For detailed statistical information, see Supplementary Table 1.

astrocytes have such a selective impact on the behavioral consequences of specific olfactory experiences? The first possibility is that deleting CB1 receptors in OB astrocytes might impair general olfactory processing. This mutation, however, did not affect odor detection or odor discrimination, and none of the OB mutants used in this study showed any impairment in body exploration. This suggests that mutant mice are able to detect and discriminate odors, both social and non-social. There is still the possibility that deletion of astrocytic mtCB1 receptors in the OB induces specific anosmia for the anogenital chemosignal(s) necessary for social transmission of stress. Specific anosmia is the inability to perceive a single odor while general olfactory processing is unchanged⁴⁴. This phenomenon mostly depends on the dysfunction of the glomeruli in charge of processing specific odors⁴⁴. There are, indeed, glomeruli that have been selectively associated with the processing of stress chemosignals⁴⁵. It seems unlikely, however, that our viral manipulations widely affecting CB1 receptor expression or MICU1 functions in astrocytes of the granular cell layer of the OB could specifically alter the activity of a limited number of glomeruli. Another possibility related to olfaction is that our manipulations might increase odor detection thresholds (hyposmia). This would imply that if the mutants spent more time with the stressed partners, they would eventually show NOR impairment. However, no correlation was found between the time spent in anogenital investigations and NOR performance. More importantly, our data indicate that, whereas a few seconds of odor exposure are sufficient to induce cognitive impairment in wild-type mice, even much longer forced contacts (>20 s) with impregnated cotton swabs do not display any effect in mutant mice. Therefore, although this possibility cannot be fully excluded at the moment, the data argue against hyposmia as a cause for the observed deficits. Thus, general regulation of olfaction seems unlikely to mediate the impact of OB astrocytic mtCB1 receptor signaling and Ca²⁺ dynamics on social transmission of stress and its cognitive consequences.

Interestingly, recent studies showed that the detection of stress chemosignals in humans is determined by mechanisms requiring only a minimal threshold exposure⁴⁶. This concept is in agreement with our observation that few seconds of exposure to a swab impregnated with anogenital secretions of a stressed partner are fully sufficient to impair cognitive performance. Therefore, rodent and human data point to the idea that social transmission of stress is likely an “all-or-none mechanism for tagging fear above a minimal threshold”⁴⁶. Astrocytes have been implicated in the processing of information in the OB¹⁷ via modulation of mitral and tufted cell activity (M/TCs)^{14–16}. Recent data indicate that OB astrocytes are under the direct control of neuromodulators such as serotonin¹⁵ or noradrenalin⁴⁷ and they can release gliotransmitters¹⁵ and control glutamate clearing^{12,16} to control neuronal activity upon odor presentation^{12,15,16}. This suggests that our manipulations of mtCB1 receptors and mitochondrial Ca²⁺ entry in astrocytes could alter the integration of olfactory information in the OB, possibly because of dysregulation of astrocyte-dependent OB circuitry. In this sense, mtCB1 receptors and mitochondrial Ca²⁺ signaling in OB astrocytes would not merely participate in the “detection” of the stress odor, but it would represent a step for its “interpretation”. Interestingly, the astrocytes in the granular cell layer appear to compartmentalize subsets of granule cells⁴⁸. The exact roles of these compartmentalized subsets are currently not known, but they have been proposed to act as functional units processing specific information⁴⁹. Indeed, granule cells were shown not only to discriminate odor identity, but also to encode their behavioral meaning⁵⁰. Thus, our data are compatible with a scenario in which astrocytic control of specific olfactory signals in the granular cell layer attributes salience to that odor. In other words, we propose that mitochondrial Ca²⁺ modulation in OB astrocytes does not impact the detection of stress signals, but it might assign specific significance to them, thereby favoring the spreading of the associated information to other parts of

the brain. Despite the fact that a short exposure to the odor is sufficient to trigger the cognitive impairment, mutant mice also display a decreased exploration of the stressed partner, possibly indicating a loss of motivation towards the specific odor as compared to wild-type animals. In summary, the present results suggest that the “salience assignment” putatively occurring in the OB and requiring control of astrocytic mitochondrial Ca²⁺ likely leads to at least two distinct effects: (i) stress-like impairment of cognition and (ii) positive reinforcement, motivating the observer to explore the partner and gather more information. Interestingly, recent work suggested that the insular cortex and its connection with the nucleus accumbens might be involved in the motivation to explore stressed conspecifics⁵¹, but no evidence exists whether these circuits are also involved in cognitive effects of odors. Thus, CB1 receptors might also modulate the activity of these higher cortical circuits. Indeed, Glu-CB1-KO mice lacking the receptor from cortical glutamatergic neurons are impaired in social behaviors towards stress partners. However, these mice have general deficits in olfaction²⁰, sociability^{52,53}, novelty seeking²² and stress responses^{54–56}, which confound the interpretation of the data. While our results on deletion of CB1 in OB neurons suggest that a local regulation via glutamatergic CB1 is not necessary for STS, future studies using genetic manipulations in specific circuits will address the interesting possibility that cortical mechanisms initiated by olfactory processes might also be under the control of the endocannabinoid system^{20,21,57,58}. Thus, by identifying one of the earliest mechanisms potentially able to assign salience to specific olfactory stimuli, the present study paves the way to investigations exploring the differences and overlaps between the circuits linking olfaction to cognitive, motivational and other behavioral processes.

Mitochondrial CB1 receptors in astrocytes have been associated to two main cellular functions: control of bioenergetic metabolism^{26,33} and regulation of mitochondrial Ca²⁺ dynamics through mitochondria/ER Ca²⁺ transfer³⁴. Whereas very little is known concerning astrocytic energy metabolism in the OB¹², solid evidence indicates that astrocytic functions in this brain region largely rely on Ca²⁺ release from internal stores^{14,59,60}. Ca²⁺ transients in astrocytes modulate olfactory-driven chemotaxis in *Drosophila*⁶¹ and M/TCs cell activity via gliotransmission in mice¹⁵. The exact role of mitochondrial Ca²⁺ signaling in OB astrocytes is unknown. However, mitochondria in astrocytes are often located close to glutamate transporters, regulating vesicular glutamate release⁶² and brain bioenergetics⁶³. Although higher resolution experiments would be required, fiber photometry results suggest that stress odors specifically increase astrocytic mitochondrial, but not cytosolic Ca²⁺ levels, possibly pointing to differential roles of subcellular compartments in the refined processing of specific odor features. Thus, our data clearly show that astrocytic mitochondrial Ca²⁺ dynamics during stress odor presentations are under the specific and direct control of mtCB1 receptors. Interestingly, MICU1 seems to exert the same control as mtCB1 receptors in STS and its cognitive consequences. Considering that the regulation of MICU1 is under the control of mtCB1 receptors³⁴, our data strongly suggest that STS and its behavioral consequences are mediated by the mtCB1 receptor-dependent regulation of mitochondrial Ca²⁺ entry by MICU1. However, we cannot exclude that these mtCB1 receptor-dependent functions might also involve mitochondrial Ca²⁺-independent processes, such as control of glycolysis and lactate signaling^{33,64} and respiratory activity^{24,33,64–66}. Interestingly, mitochondrial Ca²⁺ dynamics also regulate lactate production in astrocytes⁶⁷, suggesting the possibility that astrocytic mtCB1 receptors might be at the interplay of these cellular functions. Future studies will be needed to address the intriguing possibility that metabolic functions of astrocytic CB1 receptors might impact STS-related behaviors in combination or not with Ca²⁺ signaling.

This study shows that the processing of stress-related chemosignals in the OB during social interaction with a stressed individual

leads to an impairment of NOR, a hippocampal-dependent, non-aversive and non-olfactory cognitive test. This implies that relevant olfactory information in the OB can trigger alterations in distant circuits managing non-olfactory and non-emotional information. The nature of these circuits is not currently known, but anatomical and functional studies allow for speculation. The OB is indirectly connected with the hippocampus (HPC) through the entorhinal cortex (EC)^{68,69}, and OB oscillations play a role in the synchronization of EC-HPC activity during cognitive functions⁶⁸⁻⁷¹. Interestingly, these types of OB-EC-HPC synchronous oscillations have been observed in association with specific social odors⁷², and social transmission of stress has been recently shown to impact synaptic properties of CA1 hippocampal pyramidal neurons⁷³. Thus, functional connectivity and electrophysiological data support the possibility of an olfactory-hippocampal circuit mediating impairment of object recognition following the social transmission of stress. Moreover, corticotropin-releasing hormone (CRH) modulates anogenital investigation of stressed partners^{8,74}, and other stress-associated behaviors⁷⁵. CRH-positive neurons are spread throughout the brain, but they are particularly concentrated in the paraventricular nucleus of the hypothalamus (PVN)⁷⁶. The OB projects to the hypothalamus either indirectly through areas like the amygdala^{77,78} or even directly from specific glomeruli⁷⁹. In turn, the PVN receives indirect projections from the ventral hippocampus⁸⁰. The connections between OB, HPC and PVN could explain how CB1 receptor-dependent control of astrocytic functions in the OB and the regulation of Ca²⁺ signaling in these cells might participate in the integration of relevant olfactory cues with CRH activity and hippocampal cognitive processes.

Interestingly, olfactory pathologies suggest that altered interpretation of odor signals could be even more debilitating than complete loss of smell, particularly in the frame of social interactions. Indeed, humans living with congenital social anosmia do often compensate their complete loss of perception through other senses, such as vision and audition⁸¹. However, those living with a distortion of social chemosignaling processing (i.e. altered interpretation of detected social odors, called social dysosmia) likely suffer from deeper social deficits⁶. Thus, OB astrocytic mtCB1 receptors and mitochondrial Ca²⁺ signaling might contribute to an early specific step in the process leading from olfactory “percept” to mental “concept”, resulting in the transformation of specific cues into vital pieces of information for the organism.

The transmission of stress information in mice appears to be mediated by alarm cues similar to the odor of predators^{45,82} and, in humans, it seems that alarm- or fear-related chemosignals that are not detected within our conscious threshold are processed subconsciously, still requiring intact olfactory functions^{6,83,84}. Our results reveal a mechanistic link between social emotional odor communication and cognitive processing. Since major mental conditions like autism spectrum disorders present impairments in social olfaction⁶ and in cognitive processing^{85,86}, the present data might open novel conceptual frameworks to better tackle such conditions.

Methods

All animal protocols were in accordance with the Guidelines for the Animal Care and Use and the European Communities Council Directive of September 22th 2010 (2010/63/EU, 74) and approved by the French Ministry of Agriculture and Fisheries (authorization number 3306369) and the local ethical committee (authorization APAFIS#22372 and APAFIS #23685).

Animals

C57BL/6-N (Janvier, France) and inbred constitutive and conditional CB1 mutant (center’s facility, with a predominant C57BL/6-N background) male mice (*Mus musculus*) were used for the different experiments of this project. CB1 mutant mice included: CB1^{fl/fl} mice

(CB1-flox) carrying a floxed version of the CB1 gene³⁹; CB1-knockout mouse line (CB1-KO) carrying a constitutive global deletion of the CB1 gene³⁵; NEX-CB1-knockout mouse line (Glu-CB1-KO) carrying a conditional deletion of the CB1 gene in forebrain glutamatergic neurons under the control of a Nex-Cre recombinase³⁶; DLX-CB1 knockout mouse line (GABA-CB1-KO) carrying a conditional deletion of the CB1 gene under the control of a Dlx5/6-Cre recombinase³⁶; GFAP-Ert2-CB1-knockout mouse line (GFAP-CB1-KO) carrying an inducible conditional deletion of the CB1 gene in GFAP-expressing cells (mostly astrocytes) under the control of a GFAP-Cre recombinase²³ and a knock-in mouse line replacing the wild-type CB1 gene by a truncated form of the CB1 gene lacking the first 22 amino acids that reduces its mitochondrial-associated localization (DN22-CB1-RS)^{26,38}. The respective wild-type littermates of all lines were used as controls for the behavioral experiments.

Constitutive and inducible CB1 mutant mice were used in behavioral experiments. In the case of the GFAP-CB1-KO mice, they were injected with 8 daily injections of tamoxifen (Sigma, #T5648, 1 mg, i.p.), dissolved in 90% sesame oil, 10% ethanol to a final concentration of 10 mg/ml to induce the CreERT2 dependent CB1 gene locus excision 4 weeks before the beginning of the behavioral experiments. CB1-flox mice were used for surgical procedures to specifically assess the role of CB1 in the olfactory bulb. C57BL/6-N mice were used as demonstrators (DEM) in all behavioral experiments using surgically induced mutant mice, and for surgical procedures to assess the role of mitochondrial Ca²⁺ in astrocytes in the olfactory bulb.

Non-littermates C57BL/6-N mice coming from outside the facility and facility inbred mutant mice were housed together at 3 weeks of age (directly post weaning) in collective cages of 6-8 individuals. All animals were housed in the animal facility of Neurocentre Magendie with controlled temperature of 21 ± 2 °C, humidity 55%, in a 12 h light/12 h dark cycle (light on at 7.00am) and with water and food *ad libitum*. Animals were used at 8–17 weeks of age for the surgical and behavioral procedures, and assigned semi-randomly to experimental procedures (maintaining a balance between genotypes when required).

Adeno-associated viruses (AAV)

To generate a specific deletion on astrocytes of the OB, we used an AAV-hGFAP-Cre-IRES-mCherry purchased from the University of North Carolina (UNC School of Medicine) and an AAV-hGFAP-GFP or AAV-GFAP-dsRed as a control. To generate the specific deletion of neurons in the olfactory bulb, we used AAV-hSyn-Cre-GFP (Addgene catalog number #105540), and its control AAV-hSyn-GFP (Addgene, catalog number #105539). The AAV-CAG-Empty (used as control), AAV-CAG-DIO-CB1-GFP (expressing the wildtype CB1 construct) and AAV-CAG-DIO-DN22-GFP (expressing the DN22-CB1 construct excluding the mitochondrial associated location of the receptor) were used to specifically manipulate CB1 subcellular populations *in vivo*^{24,38}. The AAV-GFAP-mMICU1-S124A-HA-IRES-mRuby (expressing a mutated non-phosphorylatable form of the MICU1 subunit of the mitochondrial Ca²⁺ transporter) and AAV-GFAP-mMICU1-WT-HA-IRES-mRuby (expressing the wildtype version of MICU1) were used to study the effects of mitochondrial calcium dynamics *in vivo*³⁴. The AAV-GFAP-mito-GcAMP6s and AAV-GFAP-GcAMP6f were used for fiber photometry experiments³⁴. The titrations of all viruses were between 10¹⁰ and 10¹¹ genomic copies per ml for all batches.

Surgery for viral injection and fiber implantation

Mice were injected intraperitoneally with buprenorphine (0.05 mg/kg, Buprecare), sleep-induced using 5% isoflurane, and placed into a stereotaxic apparatus (Model 900, Kopf instruments, CA, USA; with mouse adaptor and lateral ear bars) using 2% isoflurane for the duration of the surgery. Local analgesia with lidocaine (0.1 ml at 0.5%, Lidor) was used under the skin of the head before incision. The viral

injections were delivered bilaterally in the olfactory bulb through a glass pipette using a microinjector (Nanolject II, Drummond Scientific). In all surgeries, mice were injected bilaterally with two injections per site of a total volume of 0.45 μ l each in the following coordinates: AP + 4.1; ML \pm 0.75; DV - 3 and - 2 at a speed of 5 nl/s.

To assess the specific contribution of astrocytic CBI receptors in the olfactory bulb to socially-transmitted stress-driven behaviors, CBI-flox mice were injected with a viral mix of two different viruses: AAV-GFAP-GFP/AAV-DIO-Empty (expressing GFP reporter protein in astrocytes as a control, Ctrl), AAV-GFAP-CRE-mCherry/AAV-DIO-Empty (generating a Cre-induced deletion of CBI receptors in GFAP positive cells, OB-GFAP-CBI-KO), AAV-GFAP-CRE-mCherry/AAV-DIO-CBI-GFP (generating both a Cre-mediated deletion of CBI receptors in astrocytes and a Cre-mediated re-expression of the wild-type construct of CBI, OB-GFAP-CBI-RS) and AAV-GFAP-CRE-mCherry/AAV-DIO-DN22-GFP (generating both a Cre-mediated deletion of CBI receptors and a Cre-mediated re-expression of the DN22-CBI construct in astrocytes, therefore re-expressing CBI everywhere but in their mitochondrial-associated locations, OB-GFAP-DN22-RS). All viruses used were titered between 2–8.10¹⁰ genomic copies/mL.

To exclude a neuronal contribution to impact on NOR of socially-transmitted stress, we injected CBI-flox mice with either an AAV-Syn-Cre-GFP or a AAV-Syn-EGFP (Ctrl) in the OB (titered 3.3.10¹¹ genomic copies/mL).

To measure in vivo Ca²⁺ calcium responses and the contribution to astrocytic CBI receptors to this process, mice were injected in the OB with either only AAV-GFAP-mitoGcAMP6s (C57BL/6-N mice); AAV-GFAP-GcAMP6f (C57BL/6-N mice) or in combination (CBI-flox mice) with AAV-GFAP-CRE-mCherry (OB-GFAP-CBI-KO), AAV-GFAP- dsRed (Ctrl). To generate the rescue and mitochondrial-specific mutants, we used mice coinjected with the GFAP-Cre and the DIO/Flex constructs AAV-DIO-CBI (OB-GFAP-CBI-RS) or the AAV-DIO-DN22 (OB-GFAP-DN22-RS). All constructs were titered 2–5.10¹¹ genomic copies/mL. Then, the optical fiber (400 μ m diameter, 0.5 NA) was placed 200 μ m above the last injection site (at DV -2, therefore at -1.8) and fixed with dental cement (MajorRepair).

To assess the contribution of mitochondrial Ca²⁺ in socially-transmitted stress, C57BL/6-N mice were injected with either AAV-GFAP-MICU^{WT} or AAV-GFAP-MICU^{S124A} in the OB (titered 3.10¹¹ genomic copies/mL).

Following surgery, all mice received i.p. injection of 0.2 ml of saline solution and anti-inflammatory drug meloxicam (5 mg/kg, Metacam), that was continued for 2 additional days. Animals continued to be housed collectively and body weight was monitored daily during 4–5 days to assess recovery. Behavioral experiments were carried out 4–5 weeks after surgery and fiber photometry experiments 5–6 weeks after surgery.

Immunostaining For Light Microscopy

AAV injected mice were deeply anesthetized with pentobarbital (400 mg/kg body weight), transcardially perfused first with 20 ml of phosphate-buffered solution (PBS 0.1 M, pH 7.4) following by 30 ml of cold 4% paraformaldehyde (Sigma, B0501128-4L). Brains were isolated and postfixed in the same fixative solution overnight at 4 °C and then transferred to a 30% (wt/vol) sucrose (Sigma, S0389) solution in PBS for cryopreservation. Brains were then frozen in isopentane (Sigma, M32631) and stored at -80 °C. Free-floating frozen sagittal sections (30 μ m) were cut using a cryostat (Leica Biosystems, CM1950S). Mid olfactory bulb slices were stored in antifreeze solution at -20 °C until further use.

Immunostaining against GFAP

Sections were washed with PBST (0.3% Triton X-100 diluted in PBS 1X pH7.4) three times and then permeabilized 1 h at room temperature (RT) in a blocking solution [in PBS 1X: 10% donkey serum; 0.3% triton

X-100]. Next, sections were incubated overnight at 4 °C with polyclonal rabbit anti-GFAP (1:1000) (Agilent, DAKO Z0334) diluted in blocking solution. After washes with PBST, brain sections were incubated for 2 h at RT with donkey anti-rabbit Alexa fluor 647 (1:500, Invitrogen) (polyc). Following washes with PBST, sections were stained with DAPI (1:20000; Invitrogen D3571), washed again with PBST and finally mounted and coverslipped.

The sections were analyzed with an epifluorescence Leica DM6000 microscope (Leica, France) to check for the intrinsic fluorescence of the viruses and the identity of the infected cells. Mouse brains that did not meet the expression requirements led to the exclusion of the mice from the experiments.

Immunostaining against GFAP and HA

Sections were washed with PBST (0.3% Triton X-100 diluted in PBS 1X pH7.4) three times and then incubated with 3% hydrogen peroxide diluted in PBST (Sigma, H1009-500ML) for 30 min. Following a step of permeabilization carried out for 1 h at RT in a blocking solution, sections were incubated overnight at 4 °C with a mix of primary antibodies: polyclonal chicken anti-GFAP (1:1000) (USBiological #G2032-25F) and monoclonal rabbit anti-HA (1:1000, Cell Signaling, 3724) diluted in blocking solution. After some washes with PBST, brain sections were incubated for 2 h at RT with a mix of secondary antibodies: goat anti rabbit IgG HRP linked antibody (Cell Signaling, 7074) and Rhodamine (TRITC) Conjugated affinitypure donkey antichick (Jackson immunoresearch, 703-025-155) (1:500). Following washes with PBST, sections were incubated with TSA plus Fluorescein (1:250) (AKOYA biosciences, NEL741001KT). Afterwards, cellular nuclei were stained with DAPI (1:20000; Invitrogen D3571), washed again with PBST and finally mounted and coverslipped.

The sections were analyzed with an epifluorescence Leica DM6000 microscope (Leica, France) to check for the intrinsic fluorescence of the viruses and the identity of the infected cells. Mouse brains that didn't meet the expression requirements led to the exclusion of the mice from the experiments. Micrographs were acquired at 10x (whole olfactory bulb) and 20x to later analyze protein co-expression.

Immunostaining For Electron Microscopy

WT and CBI-KO mice were deeply anesthetized by intraperitoneal injection of ketamine/xylazine (80/10 mg/kg body weight i.p.) and were transcardially perfused at room temperature (RT, 20–25 °C) with phosphate buffered saline (0.1 M PBS, pH 7.4) for 20 s, followed by a fixative containing 4% formaldehyde (freshly depolymerized from paraformaldehyde), 0.2% picric acid, and 0.1% glutaraldehyde in phosphate buffer (0.1 M PB, pH 7.4) for 10–15 min. Then, brains were removed from the skull and post-fixed in the same fixative for about 1 week at 4 °C. Afterwards, brains were stored at 4 °C in 1:10 diluted fixative solution until used.

Fifty μ m-thick coronal OB sections were pre-incubated in blocking solution 10% bovine serum albumin (BSA), 0.1% sodium azide and 0.02% saponine prepared in Tris-hydrogen chloride buffered saline 1x (TBS), pH 7.4 for 30 min at RT. Then, sections from both WT and CBI-KO mice were incubated with a goat anti-CBI receptor antibody (Frontier Institute Co., Ltd; goat polyclonal; CBI-Go-Af450; FR100610, 1:100) and a guinea pig polyclonal anti-GLAST antibody (Frontier Institute Co., Ltd; guinea pig polyclonal; GLAST-GP-Af1000; FR102170, 1:1,000) diluted in 10% BSA/TBS containing 0.1% sodium azide and 0.004% saponine on a shaker for 2 days at 4 °C. OB sections were incubated with 1.4 nm gold-conjugated rabbit anti-goat pig IgG antibody (Fab fragment, 1:100, #2006, Nanoprobe, Inc., Yaphank, NY, USA) and biotinylated donkey anti-guinea pig IgG antibody (1:200, 706-065-148, Jackson Immuno Research) diluted in 1% BSA/TBS 1x with 0.004% saponin on a shaker for 4 h at RT. Tissue was washed in 1% BSA/TBS 1x on a shaker at RT and incubated with ABC (1:50) prepared in

washing solution for 1.5 h at RT. Sections were rinsed with 1% BSA/TBS 1x, stored overnight at 4 °C, and post-fixed with 1% glutaraldehyde in TBS 1x (1 ml/well) for 12 min at RT. After rinsing in double distilled water, gold particles were silver-intensified with the HQ Silver kit (#2012, Nanoprobes, Inc., Yaphank, NY, USA) in the dark for 12 min at RT. The OB sections were then washed with double distilled water and 0.1 M PB (pH 7.4) for 30 minutes. The biotinylated antibody was revealed with 0.05% DAB in 0.1 M PB (pH 7.4) containing 0.5% Triton X-100 and 0.01% hydrogen peroxide for 3.5 min at RT, followed by washes in 0.1 M PB (pH 7.4). Osmication was done with 1% osmium tetroxide in 0.1 M PB (pH 7.4) in the dark for 20 min. Sections were then washed, dehydrated in graded ethanol, cleared in propylene oxide, pre-embedded in a 1:1 mix of propylene oxide/Epon 812 resin overnight at RT, and finally embedded in pure Epon 812 resin. Electron micrographs were taken with a Hamamatsu FLASH digital camera inserted in a transmission electron microscope (JEOL JEM 1400 Plus).

Behavioral protocols

Social transmission of stress. Non-littermate animals were housed together at 3 weeks of age to establish a familiarity between them while avoiding dominance issues, and then moved to new cages in couples 1–2 days before the experiment. One of the members of the couple is the demonstrator (DEM, a C57BL/6-N mouse) while the other one is the observer (OBS, depending on the experiment: [i] wild-type C57BL/6 mice, [ii] C57BL/6 mutant mice, [iii] operated C57BL/6 mice, [iv] operated C57BL/6-N) (Fig. 1a, b). As described previously⁸, the demonstrators were subjected to either a 5 min x 0.5 mA/30 s shock protocol (stress, foot-shock) in a clean fear conditioning chamber (stress DEMs), or to a 5-min separation in a novel cage (neutral) similar to the home-cage but with clean bedding (neutral DEMs), and they immediately moved back to the home-cage where they were allowed full interaction with the observer (Fig. 1a, b). Their behavior was recorded during 5 min and 8 different social and non-social behaviors were analyzed offline: anogenital exploration (snout toward the area of the congener), body exploration (all other snout contacts that are not on or near the anogenital region), allogrooming (grooming of the partner), self-grooming, digging, rearing, walking, sitting and fighting.

Odor-dependent social transmission of stress. To test whether odors were sufficient to induce transmission of stress, DEMs were habituated for three days to being swabbed on the anogenital region before the test with a clean cotton swab for 3 s, and a cotton swab was placed in the home-cage of each experimental couple for 2 days to avoid neophobia in the test. Demonstrators were swabbed with a humid cotton swab (wet with 1% saline solution) three times after the shock protocol (stress odor), or after being removed from the home-cage (neutral odor). A wet cotton swab was used as the control condition (wet swab) (Fig. 1m). Immediately after odor collection, the cotton swab was presented to the OBS in the home-cage, slightly touching their snout before dropping it on the cage bedding. Mice were allowed to interact with the cotton swab for 5 min, and then the cotton swab was removed from the cage. In the experiments of paired odor exposure and fiber photometry (Figs. 4, 5; Supplementary Fig. 4l, m, and Supplementary Fig. 6), the cotton swab was lightly maintained in front of the snout of the mouse during either 2 or 20 s before removing it from the cage.

Novel object recognition memory task. An L-shaped maze of gray PVC with two perpendicular arms placed on a white background was used in this test. The test was performed under at 50 ± 5 lux intensity with an overhung camera allowing the recording and later offline scoring of the maze exploration by the mouse.

The test consists in 3 daily phases as described previously⁸⁷. On day 1, mice were habituated to the maze for 9 min before returning to the home-cage. On day 2, they were presented with two identical

objects in each arm, and allowed to explore for 9 min to get familiar with them (acquisition phase). On day 3, mice were exposed to the maze again where one of the familiar objects is replaced by a novel one, and allowed exploration for 9 min. Exploration of an object was counted when the animal had the nose on the object or facing the object in a distance less than 0.5 cm. This phase tests the recognition performance of the animal by comparing the time spent in the novel versus the familiar objects. Object recognition capabilities are assessed by a discrimination index that is calculated by the time spent exploring the novel object minus the time spent exploring the familiar one, divided by the total exploration time. The position of the novel object and the associations of novel and familiar were randomized. All objects were previously tested to avoid biased preference. The apparatus as well as objects were cleaned with ethanol (70%) before experimental use and between each animal testing.

To test the STS effect on NOR acquisition, the couples of mice underwent the STS protocol 20 min before the acquisition phase on day 2 of the NOR test, and were tested the next day for NOR retrieval (Fig. 1i). To test the STS effect on NOR retrieval: animals underwent the STS protocol 20 min before the retrieval phase on day 3, and were subsequently tested for NOR retrieval (Fig. 1g). To study the long lasting consequences of STS, pairs of mice underwent STS on Day 3 (morning) and they were tested for NOR retrieval 6 h later (evening).

Social cognition test. Grouped house mice were habituated to an open field (30×30 cm) at 50 ± 5 lux that contained two identical cages at opposite corners, with an object inside, for 3 min. After 10 min, one of the objects was replaced by an age-matched unfamiliar mouse from the same strain, and the tested animals were allowed to interact with the cages containing object and social stimuli for 3 min (social acquisition phase). After a 10 min ITI, in which the animals underwent the STS protocol, they were moved back to the arena where the object was replaced by a novel social stimulus (age-matched unfamiliar mouse), and allowed to explore for 3 min (social novelty phase). The social discrimination index was calculated as the time spent exploring the novel social stimulus minus the time spent exploring the familiar social stimulus divided by the total time of exploration.

Buried food test. As described previously for this test⁴⁰, mice were habituated to a food pellet for 3 days in the home-cage, and food deprived for 24 h up until the test. Animals were moved to home-cage sized cages with 3–5 cm of clean bedding and allowed to roam for 10 minutes for habituation. Then, they were removed from the cages momentarily and a food pellet was hidden below the bedding at a random corner. Mice were moved back to the cage and allowed to search for the pellet for maximum 5 minutes. The time of pellet retrieval was recorded offline and if this did not occur within 5 minutes, the test was considered as failed.

Odor detection test. The experiment was performed at 50 ± 5 lux in a 35.5 × 15 × 19 cm cage that had sawdust from the home cage of the animal, with a cover that had a hole to allow easier recording. The animals were habituated during 3 days prior the test. For the habituation, a mouse was placed for 3 min in a cage that had a metal lid with a nozzle used to place a small piece of absorbent paper in it, in a way that will allow the odor impregnating the paper to diffuse, but not a direct interaction with the paper. During habituation, the piece of paper was impregnated with 10 µL of sesame oil, and the mice were subjected to 5 trials of 3 min each with 3 min inter trial, in which the mice were returned to their home cage and the paper was replaced with a similar one.

The fourth day, the test was performed. The animals were food deprived 24 hours before the test. In the test, two odors, benzaldehyde (almond) and isoamylacetate (banana) (both from Sigma Aldrich, France), were chosen to analyze the capability of detection between

different odor concentrations. In the first trial 10 μ L of sesame oil were placed under the metal cover. In the subsequent trials, 10 μ L of benzaldehyde (almond) or isoamylacetate (banana) at the concentrations 0.001%, 0.1%, 0.1% and 1% were placed under the cover, in trials 2, 3, 4 and 5, respectively. The metal cover was cleaned thoroughly between trials with ethanol 30%, so as the testing cage. The time spent sniffing the central part of the metal cover was counted offline, and counted as odor exploration while the time spent sniffing the metal cover by itself was not counted as it was assumed to be object exploration.

Odor discrimination test. The experiment was performed at 50 ± 5 lux in a new cage identical to the home-cage with clean sawdust, covered by a plexiglass with holes that allowed the exposure to a cotton swab hanging over the cage. The animals were habituated to the cage for 10 min with a wet swab. Then, the cover was quickly removed to replace the swab with a novel one with 40 μ L of benzaldehyde 0.05% (almond), and animals were allowed to explore the swab for 2 min. This was repeated two more times with new swabs, with an intertrial time of 1 min. After that, novel swabs with 40 μ L of isoamylacetate 0.05% (banana) were presented for 3 consecutive times. The time spent sniffing the swabs during the 3 minutes was counted as odor exploration.

Elevated plus maze test. The test was performed in an elevated plus maze consisting of 4 arms (height: 66 cm) of 45-cm long and 10-cm wide disposed cross-shaped and connected by a central platform of 10 cm \times 10 cm. The open arms had a light intensity of 75lux and the closed arms of 20 lx. OBS mice were placed in the open platform 20 min after social interaction with demonstrators, and allowed to explore the maze for 5 min. The time spent in open and closed arms, and the number of times they enter in those, was analyzed offline by an experimenter blind to the condition.

Social interaction with a stranger test. Experimental animals were habituated in their home-cage for 10 min to the testing room. Then, a C57BL/6-N mouse of the same sex and age was introduced in the home-cage for 5 minutes, allowing full interaction between resident and stranger. Videos of the social interaction were recorded and 8 behaviors of the resident animals towards the partners were analyzed offline: anogenital exploration, body exploration, allogroom, self-groom, digging, rearing, walking, sitting and fighting. Animals that exhibited aggressive behaviors for more than 1 min were excluded.

Fiber Photometry. Five to six weeks after surgery, freely-moving mitoGcAMP6s/cytosolic GAMP6f-expressing mice were imaged using 470 nm LED to excite the sensor, and 405 nm for the isosbestic signal control. Observer mice with fiber implants were habituated to the connection during 3 days prior the test, in 10-min sessions in which they were connected and allowed to roam in the home-cage with their familiar cage-mate. The fiber photometry set-up collected the emitted fluorescence with a sCMOS camera (Hamamatsu Orca Flash v3) through an optic fiber (core 400 μ m, N.A 0.5) divided in 2 sections: a short fiber implanted in the brain of the mouse and a long fiber (modified patchcord), both connected through a ferrule-ferrule (1.25 mm) connection. To minimize the photobleaching effect of the recording and preserve a high signal to noise ratio, the light intensities in the tip of the patch cord were adjusted to \sim 100 μ W for the 470 nm channel and \sim 50 μ W for the 405 nm channel. A custom MATLAB script (Matlabworks) was used to synchronize video recording with fiber photometry, combined with a programmed Arduino board. The sampling rate was settled at 20 Hz for both photometry (interleaved) and video recording.

On the test day, observer mice were separated from their partners for a habituation period of 5 min in which they stayed in the home-cage

while their partners were shocked (stress odor) or just separated (neutral odor) to collect the odor in a cotton swab. Observers were exposed to a cotton swab wet or the cotton swab impregnated with the partner chemosignals in an inter-individual alternated order (some mice had saline first, others the social odor first) with an interval of 4–5 min. Mice were only exposed to each odor one time, by establishing a close contact between the impregnated swab and the snout during an average time of 20 s before removing the swab from the cage. Ca^{2+} signals were recorded during the duration of the test (20 min). For non-social neutral odors odors, the animals were presented with a wet swab, a swab containing 40 μ L of isoamylacetate 0.05% (Sigma) and a swab containing benzaldehyde 0.05% (Sigma) in an inter-individual alternated order with an interval of 4–5 min, while mitochondrial calcium changes were recorded.

Raw calcium Ca^{2+} were pre-processed by removing the first minute of the recording to decrease the effect of the first exponential photobleaching, and by removing point artifacts. The 470 nm signal was fitted to the isosbestic 405 nm using a polynomial fit of first degree and, for each time point, $\Delta F/F$ was calculated as $(F_{470nm} - F_{405nm}(\text{fitted}))/F_{405nm}(\text{fitted})$. $\Delta F/F$ values were smoothed using a moving average of 0.5 s. Z-score was calculated in the whole recording to take into account the changes in signal intensity during the experiments. The signal corresponding to 1 min after the onset of the odor exposure was extracted, with 15 s baseline before the onset. The baseline values were used to correct the extracted signal by performing a subtraction of the mean of the baseline to the whole extracted signal. The area under the curve during the 20 s of swab exposure of the odors was calculated from the z-scored data. Ca^{2+} signals from wet swab and the different odors were compared within mice.

Quantification and statistical analysis

Data collection. All data points that appear in the graphs of this study correspond to individual sample mice, and not technical replicates. Statistical methods to determine sample size were not used, but the numbers of animals used were similar to those in the literature. Experimenters analyzing the raw videos were always blind to the conditions of the subject. All mice were randomly assigned to experimental conditions. We used custom software to analyze the social behaviors and time spent in each arm during the novel object recognition. For the analysis of the immunostaining, we used Fiji. The contrast and brightness parameters were adjusted and applied equally to all micrographs. Fiji's cell counter plug-in was used to establish overlap between differently expressed proteins. For the fiber photometry data, we extracted the signal as described above using the provided custom code. Raw data from all experiments was processed and analyzed using Microsoft Excel 2020 and Graph Pad 8.0.

Statistical analysis

Graphs and statistical analysis were performed with Graph Pad 8.0. All data come from distinct samples (individual mice) and they are shown as independent data points per animal \pm standard error of the mean (SEM). Each experiment was repeated with at least two independent batches. Normality of the data was assessed with the Kolmogorov-Smirnoff test for all sample sizes >5 or Shapiro-Wilk test for sample sizes <5 , and, depending on the result, parametric (paired and unpaired Student's *t* test, ordinary one-way ANOVA with Bonferroni post hoc analysis, or ordinary two-way ANOVA when necessary) or non-parametric (unpaired Mann-Whitney test, Wilcoxon matched pairs signed rank test or Kruskal-Wallis test with Dunn's post hoc analysis) were performed. Detailed statistical data for each experiment including exact mean \pm SEM values, test statistic with confidence intervals, group sizes, degrees of freedom and exact *P* values can be found in Supplementary Table 1 (for main Figures) and Supplementary Table 2 (for Supplementary Figs.).

Reporting summary

Further information on research design is available in the Nature Portfolio Reporting Summary linked to this article.

Data availability

The data generated in this study are provided in the Source Data file. Sequences of non-commercial plasmids will be provided upon request. Source data are provided with this paper.

Code availability

The codes used for the analysis of the fiber photometry experiments in this study can be found in: <https://github.com/TeamMarsicano/Gomez-Sotres-et-al-2024>: <https://doi.org/10.5281/zenodo.13122660>.

References

- Chen, D., Katdare, A. & Lucas, N. Chemosignals of fear enhance cognitive performance in humans. *Chem. Senses* **31**, 415–423 (2006).
- Mutic, S., Br nner, Y. F., Rodriguez-Raecke, R., Wiesmann, M. & Freiherr, J. Chemosensory danger detection in the human brain: Body odor communicating aggression modulates limbic system activation. *Neuropsychologia* **99**, 187–198 (2017).
- Dalton, P., Maut , C., Ja n, C. & Wilson, T. Chemosignals of stress influence social judgments. *PLoS One* **8**, e77144 (2013).
- de Groot, J. H. B., Smeets, M. A. M. & Semin, G. R. Rapid stress system drives chemical transfer of fear from sender to receiver. *PLoS One* **10**, e0118211 (2015).
- de Groot, J. H. B. et al. A sniff of happiness. *Psychol. Sci.* **26**, 684–700 (2015).
- Endevelt-Shapira, Y. et al. Altered responses to social chemosignals in autism spectrum disorder. *Nat. Neurosci.* **21**, 111–122 (2018).
- Kiyokawa, Y., Kikusui, T., Takeuchi, Y. & Mori, Y. Alarm pheromones with different functions are released from different regions of the body surface of male rats. *Chem. Senses* **29**, 35–40 (2004).
- Sterley, T. L. et al. Social transmission and buffering of synaptic changes after stress. *Nat. Neurosci.* **21**, 393–403 (2018).
- Dorey, R., Pi rard, C., Chauveau, F., David, V. & B racoch a, D. Stress-induced memory retrieval impairments: different time-course involvement of corticosterone and glucocorticoid receptors in dorsal and ventral hippocampus. *Neuropsychopharmacology* **37**, 2870–2880 (2012).
- Busquets-Garcia, A. et al. Peripheral and central CB1 cannabinoid receptors control stress-induced impairment of memory consolidation. *Proc. Natl. Acad. Sci. USA* **113**, 9904–9909 (2016).
- Skupio, U. et al. Mitochondrial cannabinoid receptors gate corticosterone impact on novel object recognition. *Neuron* **111**, 1887–1897.e6 (2023).
- Martin, C. et al. Alteration of sensory-evoked metabolic and oscillatory activities in the olfactory bulb of GLAST-deficient mice. *Front. Neural Circuits* **6**, 1 (2012).
- Roux, L., Benchenane, K., Rothstein, J. D., Bonvento, G. & Giaume, C. Plasticity of astroglial networks in olfactory glomeruli. *Proc. Natl. Acad. Sci. USA* **108**, 18442–18446 (2011).
- Roux, L. et al. Astroglial connexin 43 hemichannels modulate olfactory bulb slow oscillations. *J. Neurosci.* **35**, 15339–15352 (2015).
- Sardar, D. et al. Induction of astrocytic Slc22a3 regulates sensory processing through histone serotonylation. *Science* **380**, eade0027 (2023).
- Ung, K. et al. Olfactory bulb astrocytes mediate sensory circuit processing through Sox9 in the mouse brain. *Nat. Commun.* **12**, 5230 (2021).
- Ung, K., Tepe, B., Pekarek, B., Arenkiel, B. R. & Deneen, B. Parallel astrocyte calcium signaling modulates olfactory bulb responses. *J. Neurosci. Res.* **98**, 1605–1618 (2020).
- Busquets-Garcia, A. et al. Dissecting the cannabinergic control of behavior: The where matters. *BioEssays* **37**, 1215–1225 (2015).
- Terral, G. et al. CB1 receptors in the anterior piriform cortex control odor preference memory. *Curr. Biol.* **29**, 2455–2464.e5 (2019).
- Soria-G mez, E. et al. The endocannabinoid system controls food intake via olfactory processes. *Nat. Neurosci.* **17**, 407–415 (2014).
- Terral, G. et al. Endogenous cannabinoids in the piriform cortex tune olfactory perception. *Nat. Commun.* **15**, 1230 (2024).
- Laf n tre, P., Chaouloff, F. & Marsicano, G. Bidirectional regulation of novelty-induced behavioral inhibition by the endocannabinoid system. *Neuropharmacology* **57**, 715–721 (2009).
- Han, J. et al. Acute cannabinoids impair working memory through astroglial CB1 receptor modulation of hippocampal LTD. *Cell* **148**, 1039–1050 (2012).
- Hebert-Chatelain, E. et al. A cannabinoid link between mitochondria and memory. *Nature* **539**, 555–559 (2016).
- Wang, Z. J. et al. Cannabinoid receptor-mediated modulation of inhibitory inputs to mitral cells in the main olfactory bulb. *J. Neurophysiol.* **122**, 749–759 (2019).
- Wang, Z. J., Sun, L. & Heinbockel, T. Cannabinoid receptor-mediated regulation of neuronal activity and signaling in glomeruli of the main olfactory bulb. *J. Neurosci.* **32**, 8475–8479 (2012).
- Heinbockel, T. & Straiker, A. Cannabinoids regulate sensory processing in early olfactory and visual neural circuits. *Front. Neural Circuits* **15**, 662349 (2021).
- Navarrete, M. & Araque, A. Endocannabinoids mediate neuron-astrocyte communication. *Neuron* **57**, 883–893 (2008).
- Guti rrez-Rodr guez, A. et al. Localization of the cannabinoid type-1 receptor in subcellular astrocyte compartments of mutant mouse hippocampus. *Glia* **66**, 1417–1431 (2018).
- Robin, L. M. et al. Astroglial CB1 receptors determine synaptic D-serine availability to enable recognition memory. *Neuron* **98**, 935–944.e5 (2018).
- Covelo, A. & Araque, A. Lateral regulation of synaptic transmission by astrocytes. *Neuroscience* **323**, 62–66 (2016).
- B nard, G. et al. Mitochondrial CB1 receptors regulate neuronal energy metabolism. *Nat. Neurosci.* **15**, 558–564 (2012).
- Jimenez-Blasco, D. et al. Glucose metabolism links astroglial mitochondria to cannabinoid effects. *Nature* **583**, 603–608 (2020).
- Serrat, R. et al. Astroglial ER-mitochondria calcium transfer mediates endocannabinoid-dependent synaptic integration. *Cell Rep.* **37**, 110133 (2021).
- Marsicano, G. et al. The endogenous cannabinoid system controls extinction of aversive memories. *Nature* **418**, 530–534 (2002).
- Monory, K. et al. The endocannabinoid system controls key epileptogenic circuits in the hippocampus. *Neuron* **51**, 455–466 (2006).
- Han, J. et al. Acute cannabinoids impair working memory through astroglial CB1 receptor modulation of hippocampal LTD. *Cell* **148**, 1039–1050 (2012).
- Soria-Gomez, E. et al. Subcellular specificity of cannabinoid effects in striatonigral circuits. *Neuron* **109**, 1513–1526.e11 (2021).
- Marsicano, G. et al. CB1 cannabinoid receptors and on-demand defense against excitotoxicity. *Science* **302**, 84–88 (2003).
- Machado, C. F., Reis-Silva, T. M., Lyra, C. S., Felicio, L. F. & Malnic, B. Buried food-seeking test for the assessment of olfactory detection in mice. *Bio-protocol* **8**, e2897 (2018).
- Rizzuto, R., De Stefani, D., Raffaello, A. & Mammucari, C. Mitochondria as sensors and regulators of calcium signalling. *Nat. Rev. Mol. Cell Biol.* **13**, 566–578 (2012).
- Mallilankaraman, K. et al. MICU1 is an essential gatekeeper for MCU-mediated mitochondrial Ca²⁺ uptake that regulates cell survival. *Cell* **151**, 630 (2012).
- Marchi, S. et al. Akt-mediated phosphorylation of MICU 1 regulates mitochondrial Ca²⁺ levels and tumor growth. *EMBO J.* **38**, (2019).

44. Niimura, Y. Olfactory receptor multigene family in vertebrates: From the viewpoint of evolutionary genomics. *Curr. Genomics* **13**, 103 (2012).
45. Brechbühl, J., Klaey, M. & Broillet, M.-C. Grueneberg ganglion cells mediate alarm pheromone detection in mice. *Science* **321**, 1092–1095 (2008).
46. de Groot, J. H. B., Kirk, P. A. & Gottfried, J. A. Titrating the smell of fear: initial evidence for dose-invariant behavioral, physiological, and neural responses. *Psychol. Sci.* **32**, 558–572 (2021).
47. Fischer, T., Prey, J., Eschholz, L., Rotermund, N. & Lohr, C. Norepinephrine-induced calcium signaling and store-operated calcium entry in olfactory bulb astrocytes. *Front. Cell. Neurosci.* **15**, 639754 (2021).
48. Bailey, M. S. & Shipley, M. T. Astrocyte subtypes in the rat olfactory bulb: Morphological heterogeneity and differential laminar distribution. *J. Comp. Neurol.* **328**, 501–526 (1993).
49. Reyher, C. K. H. et al. Olfactory bulb granule cell aggregates: morphological evidence for interperikaryal electrotonic coupling via gap junctions. *J. Neurosci.* **11**, 1485–1495 (1991).
50. Wang, D. et al. Improved separation of odor responses in granule cells of the olfactory bulb during odor discrimination learning. *Front. Cell. Neurosci.* **14**, 579349 (2020).
51. Rogers-Carter, M. M., Djerdjaj, A., Gribbons, K. B., Varela, J. A. & Christianson, J. P. Insular cortex projections to nucleus accumbens core mediate social approach to stressed juvenile rats. *J. Neurosci.* **39**, 8717–8729 (2019).
52. Häring, M., Kaiser, N., Monory, K. & Lutz, B. Circuit specific functions of cannabinoid CB1 receptor in the balance of investigatory drive and exploration. *PLoS One* **6**, e26617 (2011).
53. Jacob, W. et al. Endocannabinoids render exploratory behaviour largely independent of the test aversiveness: role of glutamatergic transmission. *Genes. Brain. Behav.* **8**, 685–698 (2009).
54. Metna-Laurent, M. et al. Bimodal control of fear-coping strategies by CB1 cannabinoid receptors. *J. Neurosci.* **32**, 7109–7118 (2012).
55. Kamprath, K. et al. Endocannabinoids mediate acute fear adaptation via glutamatergic neurons independently of corticotropin-releasing hormone signaling. *Genes, Brain Behav.* **8**, 203–211 (2009).
56. Steiner, M. A., Marsicano, G., Wotjak, C. T. & Lutz, B. Conditional cannabinoid receptor type 1 mutants reveal neuron subpopulation-specific effects on behavioral and neuroendocrine stress responses. *Psychoneuroendocrinology* **33**, 1165–1170 (2008).
57. Zhao, Z. et al. Cannabinoids regulate an insula circuit controlling water intake. *Curr. Biol.* **34**, 1918–1929.e5 (2024).
58. Rieger, N. S. et al. Insular cortex corticotropin-releasing factor integrates stress signaling with social affective behavior. *Neuropsychopharmacology* **47**, 1156 (2022).
59. Doengi, M., Deitmer, J. W. & Lohr, C. New evidence for purinergic signaling in the olfactory bulb: A2A and P2Y1 receptors mediate intracellular calcium release in astrocytes. *FASEB J.* **22**, 2368–2378 (2008).
60. Petzold, G. C., Albeanu, D. F., Sato, T. F. & Murthy, V. N. Coupling of neural activity to blood flow in olfactory glomeruli is mediated by astrocytic pathways. *Neuron* **58**, 897–910 (2008).
61. Ma, Z., Stork, T., Bergles, D. E. & Freeman, M. R. Neuromodulators signal through astrocytes to alter neural circuit activity and behaviour. *Nature* **539**, 428–432 (2016).
62. Reyes, R. C. & Parpura, V. Mitochondria modulate Ca²⁺-dependent glutamate release from rat cortical astrocytes. *J. Neurosci.* **28**, 9682 (2008).
63. Robinson, M. B. & Jackson, J. G. Astroglial glutamate transporters coordinate excitatory signaling and brain energetics. *Neurochem. Int.* **98**, 56–71 (2016).
64. Fernández-Moncada, I. et al. A lactate-dependent shift of glycolysis mediates synaptic and cognitive processes in male mice. *Nat. Commun.* **15**, 6842 (2024).
65. Suzuki, A. et al. Astrocyte-neuron lactate transport is required for long-term memory formation. *Cell* **144**, 810–823 (2011).
66. Descalzi, G., Gao, V., Steinman, M. Q., Suzuki, A. & Alberini, C. M. Lactate from astrocytes fuels learning-induced mRNA translation in excitatory and inhibitory neurons. *Commun. Biol.* **21**, 1–11 (2019).
67. Cabral-Costa, J. V. et al. Mitochondrial sodium/calcium exchanger NCLX regulates glycolysis in astrocytes, impacting on cognitive performance. *J. Neurochem.* <https://doi.org/10.1111/JNC.15745> (2022).
68. Gourévitch, B., Kay, L. M. & Martin, C. Directional coupling from the olfactory bulb to the hippocampus during a go/no-go odor discrimination task. *J. Neurophysiol.* **103**, 2633–2641 (2010).
69. Martin, C., Beshel, J. & Kay, L. M. An olfacto-hippocampal network is dynamically involved in odor-discrimination learning. *J. Neurophysiol.* **98**, 2196–2205 (2007).
70. Salimi, M. et al. The olfactory bulb modulates entorhinal cortex oscillations during spatial working memory. *J. Physiol. Sci.* **71**, (2021).
71. Salimi, M. et al. Disrupted connectivity in the olfactory bulb-entorhinal cortex-dorsal hippocampus circuit is associated with recognition memory deficit in Alzheimer’s disease model. *Sci. Rep.* **12**, (2022).
72. Pena, R. R. et al. Home-cage odors spatial cues elicit theta phase/gamma amplitude coupling between olfactory bulb and dorsal hippocampus. *Neuroscience* **363**, 97–106 (2017).
73. Lee, I. C., Yu, T. H., Liu, W. H. & Hsu, K. Sen. Social Transmission and Buffering of Hippocampal Metaplasticity after Stress in Mice. *J. Neurosci.* **41**, 1317–1330 (2021).
74. Rogers-Carter, M. M. et al. Insular cortex mediates approach and avoidance responses to social affective stimuli. *Nat. Neurosci.* **21**, 404–414 (2018).
75. Füzesi, T., Daviu, N., Wamsteeker Cusulin, J. I., Bonin, R. P. & Bains, J.S. Hypothalamic CRH neurons orchestrate complex behaviours after stress. *Nat. Commun.* **7**, 11937 (2016).
76. Cui, Z., Gerfen, C. R. & Young, W. S. Hypothalamic and other connections with dorsal CA2 area of the mouse hippocampus. *J. Comp. Neurol.* **521**, 1844–1866 (2013).
77. Lin, W., Margolskee, R., Donnert, G., Hell, S. W. & Restrepo, D. Olfactory neurons expressing transient receptor potential channel M5 (TRPM5) are involved in sensing semiochemicals. *Proc. Natl. Acad. Sci. USA* **104**, 2471–2476 (2007).
78. Thompson, J. A., Salcedo, E., Restrepo, D. & Finger, T. E. Second-order input to the medial amygdala from olfactory sensory neurons expressing the transduction channel TRPM5. *J. Comp. Neurol.* **520**, 1819–1830 (2012).
79. Bader, A., Klein, B., Breer, H. & Strotmann, J. Connectivity from OR37 expressing olfactory sensory neurons to distinct cell types in the hypothalamus. *Front. Neural Circuits* **6**, 84 (2012).
80. Cole, A. B., Montgomery, K., Bale, T. L. & Thompson, S. M. What the hippocampus tells the HPA axis: Hippocampal output attenuates acute stress responses via disynaptic inhibition of CRF+ PVN neurons. *Neurobiol. Stress* **20**, 100473 (2022).
81. Lemogne, C. et al. Congenital anosmia and emotion recognition: A case-control study. *Neuropsychologia* **72**, 52–58 (2015).
82. Brechbühl, J. et al. Mouse alarm pheromone shares structural similarity with predator scents. *Proc. Natl. Acad. Sci. USA* **110**, 4762–4767 (2013).
83. Albrecht, J. et al. Smelling chemosensory signals of males in anxious versus nonanxious condition increases state anxiety of female subjects. *Chem. Senses* **36**, 19–27 (2011).
84. de Groot, J. H. B., Smeets, M. A. M., Kaldewaij, A., Duijndam, M. J. A. & Semin, G. R. Chemosignals communicate human emotions. *Psychol. Sci.* **23**, 1417–1424 (2012).
85. Okumura, T., Kumazaki, H., Singh, A. K., Touhara, K. & Okamoto, M. Individuals with autism spectrum disorder show altered event-

- related potentials in the late stages of olfactory processing. *Chem. Senses* **45**, 45–58 (2020).
86. Gaigg, S. B. The interplay between emotion and cognition in Autism Spectrum Disorder: Implications for developmental theory. *Front. Integrative Neurosci.* **6** <https://doi.org/10.3389/fnint.2012.00113> (2012).
87. Da Cruz, J. F. O. et al. An alternative maze to assess novel object recognition in mice. *Bio-Protoc.* **10**, e3651 (2020).

Acknowledgements

We would like to thank Delphine Gonzales, Nathalie Aubailly, Ruby Racunica, Jean-Baptiste Bernard and all the personnel of the Animal Facilities of the NeuroCentre Magendie for mouse care. We also thank the genotyping platform of the Neurocentre Magendie for the help in the experiments. The microscopy was done in the Bordeaux Imaging Center a service unit of the CNRS-INSERM and Bordeaux University, member of the national infrastructure France Biolmaging supported by the French National Research Agency (ANR-10-INBS-04). We thank all the members of Marsicano's lab for useful discussions and for their invaluable support. We thank Toni-Lee Sterley and Tamas Fuzesi for providing the software to analyze social behaviors and their valuable input in the analysis. This study was funded by Inserm (to G.M.); the European Research Council (Micabra, ERC-2017-AdG-786467, to G.M.); Fondation pour la Recherche Medicale (DRM20101220445, to G.M.; SPF201809006908 to U.S.); the Human Frontiers Science Program (to G.M.); Region Aquitaine (CanBrain, AAP2022A-2021-16763610 and -17219710 to G.M.); French State/Agence Nationale de la Recherche (ERA-Net Neuron CanShank, ANR-21-NEU2-0001-04, to G.M), (CaMeLS, ANR-23-CE16-0022-01, to G.M), (Hippobese, ANR-23-CE14-0004-03, to G.M); the French government in the framework of the University of Bordeaux IdEx "Investments for the Future" program / GPR BRAIN_2030 (to P.G-S and G.M) and Bordeaux Collaboration Scheme (to P.G-S); La Caixa Research Health grant HR23-00793 (to G.M. and A. B-G); the Canadian Institutes for Health and Research (FDN-148440 to J.S.B); The Basque Government (IT1620-22 to P.G); Atención Primaria, Cronicidad y Promoción de la Salud, Red de Investigación en Atención Primaria de Adicciones (RIAPAd), Instituto de Salud Carlos III (RD21/0009/0006 to P.G)

Author contributions

P. G.-S. contributed to the conception of the project and performed and analyzed all experiments. U.S. helped with the conception and performance of some behavioral experiments. T.D. and F.D. helped in behavioral experiments. F.J.-K. and D.G. performed immunohistochemistry assays. I.B.R, P.G. and N.P performed the electron microscopy experiments. A.C. and L.B. generated plasmids and adeno-associated viruses. A.B.-G. contributed to the conception of

the study both theoretically and with behavioral experiments. P.G.-S., J.S.B. and G.M. wrote the manuscript. All authors edited the manuscript. This project arises from a conceptual combination effort between J.S.B. and G.M. who conceived and supervised the whole project together, and whose expertise was equally important, justifying the presence of two senior authors.

Competing interests

The authors declare no competing interests.

Additional information

Supplementary information The online version contains supplementary material available at <https://doi.org/10.1038/s41467-024-51416-4>.

Correspondence and requests for materials should be addressed to Jaideep S. Bains or Giovanni Marsicano.

Peer review information *Nature Communications* thanks Carmen Sandi, who co-reviewed with Silvie Ruigrok, and the other, anonymous, reviewer(s) for their contribution to the peer review of this work. A peer review file is available.

Reprints and permissions information is available at <http://www.nature.com/reprints>

Publisher's note Springer Nature remains neutral with regard to jurisdictional claims in published maps and institutional affiliations.

Open Access This article is licensed under a Creative Commons Attribution-NonCommercial-NoDerivatives 4.0 International License, which permits any non-commercial use, sharing, distribution and reproduction in any medium or format, as long as you give appropriate credit to the original author(s) and the source, provide a link to the Creative Commons licence, and indicate if you modified the licensed material. You do not have permission under this licence to share adapted material derived from this article or parts of it. The images or other third party material in this article are included in the article's Creative Commons licence, unless indicated otherwise in a credit line to the material. If material is not included in the article's Creative Commons licence and your intended use is not permitted by statutory regulation or exceeds the permitted use, you will need to obtain permission directly from the copyright holder. To view a copy of this licence, visit <http://creativecommons.org/licenses/by-nc-nd/4.0/>.

© The Author(s) 2024